



NORSE 2023
R/V KRONPRINS HAAKON
6-30 NOVEMBER
CRUISE REPORT



Table of Contents (clickable!)

| | |
|--|-----------|
| 1. Scientific Motivation | 3 |
| 2. Working with the Kronprins Haakon | 3 |
| 3. Cruise Overview and Timeline | 4 |
| 4. Instruments and Methodology | 5 |
| Mooring Recovery. | 5 |
| DBASIS System | 6 |
| Shipboard Profiling | 7 |
| Shipboard CTD and Lowered ADCP | 8 |
| V-Wing | 9 |
| Bow Chain | 10 |
| Gliders | 11 |
| Floats and Drifters | 15 |
| Sound source from the ship | 19 |
| 5. Preliminary Results | 20 |
| Overview | 20 |
| Meteorological conditions | 21 |
| Stirring and subduction, spice and subsurface heat maxima near Jan Mayen | 22 |
| Acoustics: submesoscale upper ocean structure around Jan Mayen | 29 |
| Strong Surface Forcing and SWIFT Wind/Wave measurements | 31 |
| Little whorls have lesser whorls: finescale and microscale phenomenology | 36 |
| The end of the cascade: turbulent mixing | 39 |
| Larger scale context: circumnavigation of Jan Mayen | 40 |
| Looking deeper: Shipboard CTD and Lowered ADCP measurements | 41 |
| Lofoten Basin Eddy | 42 |
| Year-long records: Acoustics | 44 |
| Year-long record: Physical Oceanography | 47 |
| Internal tides near Jan Mayen Ridge | 49 |
| Larger-scale context: Glider Freya Transit from Iceland | 51 |
| Larger-scale context: Wave Glider Ole Transit from Iceland | 53 |
| 6. Educational activities during the cruise | 54 |
| 7. Science Party Personnel | 54 |
| 8. Appendix | 55 |
| Detailed Schedule | 55 |
| Swift Deployments | 58 |
| CTD/LADCP stations: | 58 |
| Bow Chain Deployments | 58 |
| V-Wing Deployments | 59 |

The Office of Naval Research Northern Ocean Rapid Surface Evolution (NORSE) Departmental Research Initiative (DRI) focuses on characterizing the key physical parameters and processes that govern the predictability of upper-ocean rapid evolution events occurring in the ice-free high latitudes. The goal is to identify which observable parameters are most influential in improving model predictability through inclusion by assimilation, and to field an autonomous observing network that optimizes sampling of high-priority fields. The objective is to demonstrate improvements in the predictability of the upper ocean physical fields associated with acoustic propagation over the course of the study.

1. Scientific Motivation

The main objectives of the 2023 NORSE fieldwork were to understand and develop knowledge on how to predict the changes in acoustic propagation across ranges of less than 100 km, over time scales of a few days, particularly around times when the ocean changes rapidly (e.g., storms). The governing questions include both those that are primarily physical oceanography questions and those that are primarily acoustics questions: the crux of this experiment is the unique ability to look at how these physical oceanography and acoustics questions are intertwined and interdependent.

The ship-anchored fieldwork was centered around the Jan Mayen area, where warm salty Atlantic waters meet cooler fresher polar waters from the Greenland Basin. This year there was a particularly rich and complicated ‘soup’ of intermediate water masses between the two end points, full of submesoscale eddies that facilitate stirring, subduction and mixing of these waters. The result was an intricate pattern of sound speed and sub-surface acoustic ducts. Modest winds during the first part of the fieldwork allowed these lateral and vertical gradients to extend nearly all the way to the surface. A strong storm during the last week allowed us the opportunity to look at how strong surface forcing played out similarly and differently at various points in this stratification pattern. Here we present an overview of cruise activities, technical accomplishments and preliminary scientific results.

2. Working with the Kronprins Haakon

This was our first experience working the the Kronprins Haakon (KPH). We found it to be a remarkably capable ship. The physical facilities were top notch, the captain and crew were helpful at every opportunity, the ship rode amazingly well in rough weather, and all of our operations went smoothly. We especially appreciated the extra efforts to make us feel at home, from frequent check-ins leading up to the cruise to vegan meals. We would highly recommend the ship be considered for future work in the region.

3. Cruise Overview and Timeline

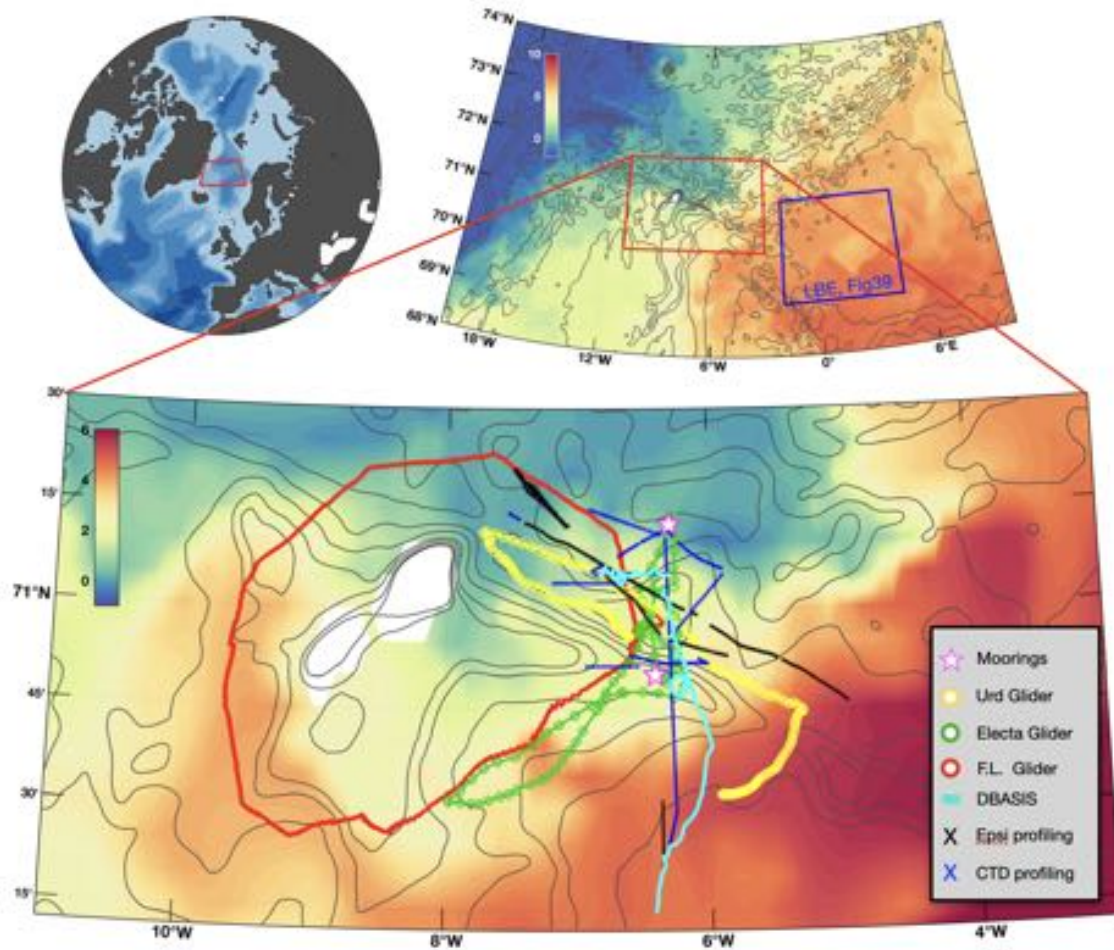


Figure 1: Map of a subset of Norse 2023 sampling (numerous drifters not included, for clarity). Sea-Surface Temperature in the background, in °C, is from the Barrents 2.5 Norwegian model, which was remarkably accurate.

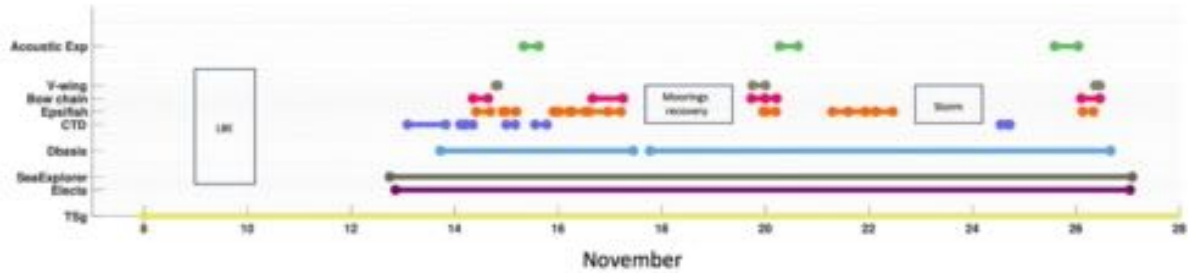


Figure 2: Gantt chart of cruise activities

4. Instruments and Methodology

Here we present details of the scientific instrumentation and associated procedures.

Mooring Recovery.

A primary goal of this expedition was the safe recovery of the moorings deployed in October 2022. All four moorings were successfully recovered over a two period on November 18 and 19.

The PECOS array functioned all year and continued its scheduled recordings until we picked it up on 18 November 2023. During the yearlong recording, we only lost two of 52 channels: channel 29 was lost on 2 January and channel 24 degraded around 16 July. However, upon examination of the acoustic data recorded by the PECOS array, we learned the moored source stopped broadcasting on 13 November 2022 after its 0800 UTC transmission. Examination of the source identifies the failure point was the chip-scale atomic clock (CSAC). The transducer is still functional, and the microcontroller responds when queried, but the CSAC is unresponsive. We are working with the vendor to investigate why this failure occurred.

The PECOS array was outfitted with four RBR duets and four MAT1 tilt sensors. All of these sensors functioned through the experiment and provide an annual record of the temperature profile between 50 and 400 m. The PECOS array experienced some blowdown, with a maximum excursion of 36 m recorded at 100 m depth during a high current event 25 December 2022. The source mooring included one RBR duet, one MAT1, two SBE37s, and 12 SBE56s. The RBR duet, MAT1, and SBE37s functioned throughout the year, but 11 of the 12 SBE56s stopped working during the experiment, and all the SBE56s below 100m stopped providing temperature data between mid-January and mid-February 2023. The source mooring was very stable with a maximum depth excursion of 4 m

recorded at 100 m depth on 18 May 2023.

The shallow water environmental mooring was recovered on 18 November 2023. The Nortek signature 500, workhorse sentinel, long ranger and SBEs successfully recorded throughout the deployment. The rbr thermistors ran out of battery during July 2023. The SWE mooring experienced the same blow down as the PECOS mooring on 25 December 2023, with a vertical excursion to 100 m (70 m difference). The pitch and roll from the WHS suggests the stablemoor was successful at stabilizing the ADCPs during these events.

The UiB environmental mooring was recovered on 19 November 2023. The 1500m deep mooring was equipped with: RDI 300kHz ADCP, RDI 75kHz ADCP, Nortek S100 ADCP, Nortek S55 ADCP, two SeaGuard RCM with CTD, two SBE39, seven SBE37, and thirteen SBE56. Apart from one SBE37 (sn 7222), which had a malfunctioning pressure sensor, all SBEs measured as scheduled throughout the yearlong deployment. The top ~300m of the UiB mooring also experienced the same blowdown as the PECOS and shallow water environmental mooring.

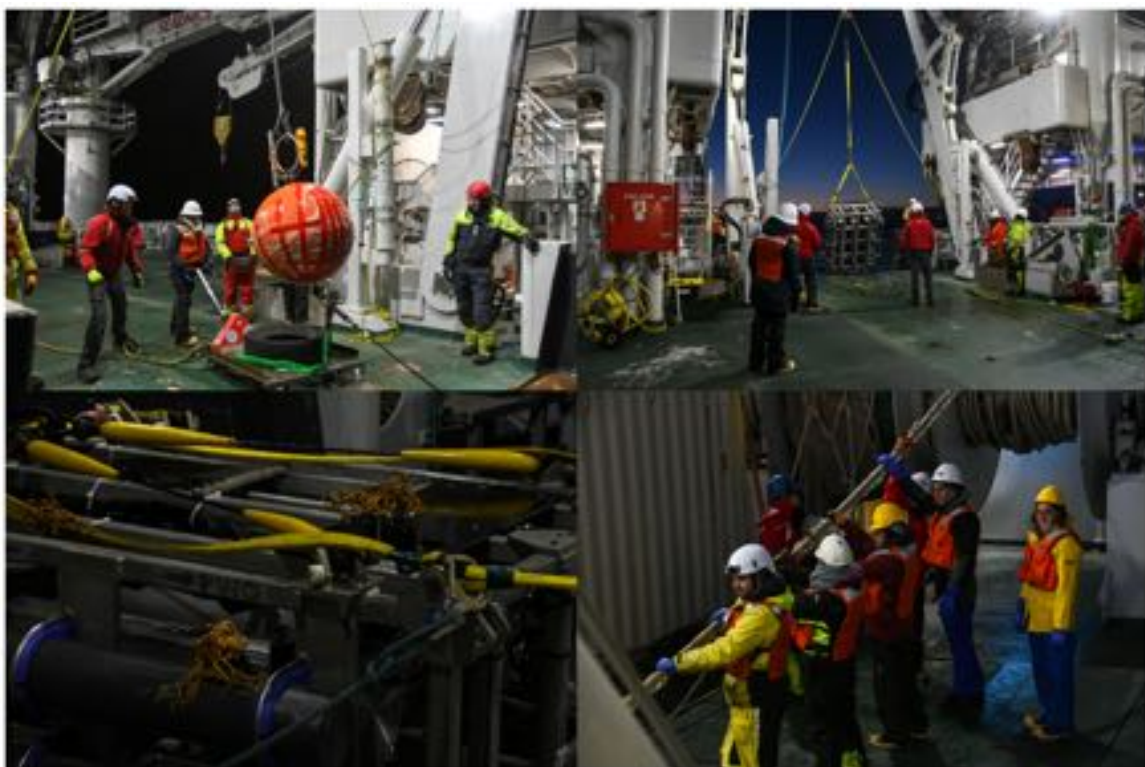


Figure 3: PECOS array recovery on 18 November 2023.

DBASIS System

The DBASIS developed from a SIO/WHOI collaboration involving the integration of a WHOI air-sea flux buoy with a SIO Wirewalker vertical profiling vehicle. DBASIS buoys measure the bulk air-sea fluxes and the response of the ocean boundary layer simultaneously in real time and in high resolution. The DBASIS system was deployed on 13 November and recovered 26 November.. The top Wirewalker was slightly under-ballasted, resulting in slow upward profiles and some stalling at the top stop. To address these issues, the DBASIS system was recovered, reballasted, and redeployed 17 November. It was recovered from the second deployment on 26 November . During the storm, some buoys sensors iced over resulting in temporary data dropouts. Over the course of both deployments there were 3723 wirewalker profiles overall split between two wirewalkers.

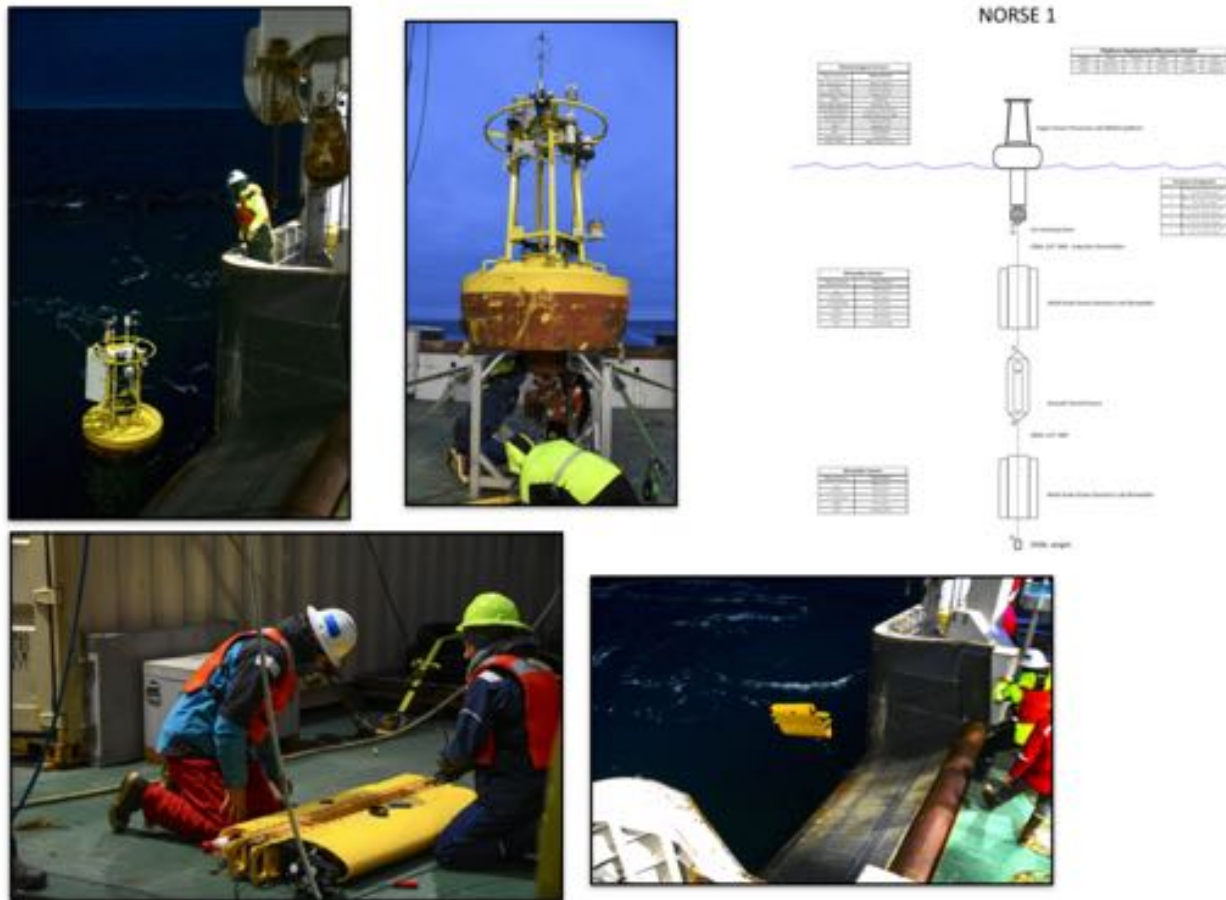


Figure 4: Upper Right schematic showing the components of the DBASIS buoy as deployed on IOP1. Others: Photos from the 2023 deployment.

Shipboard Profiling

We profiled from the stern using a commercial fishing reel winch and 500 lb spectra line. We had two profiling vehicles, the Epsi Minnow and an RBR concerto with a tridente and DO sensor. The Epsi Minnow has two shear probes and two FPO7 high resolution temperature probes as well as a SBE 49. We included a 8m shot of $\frac{1}{4}$ " spectra between the end of the fishing reel line and the top of the profiling vehicle. This allowed us to lower the vehicles by hand or use the block that we set up above the pick up point. We would pull the $\frac{1}{4}$ " spectra through the block and avoid pulling the fishing reel line through. Watch standers stood one hour rotating shifts where two people would be on deck operating the fishing reel. We had two Epsi Minnows on board and were able to swap them out every 6 hours in order to download data, change probes, recharge batteries, etc. while keeping a continuous profiling line.

Overall there were 522 profiles with CTD data, 245 of which also contained microstructure data.



Figure 5: Clockwise from top-left: Winch and deployment boom for the Epsi Minnow and RBR profiling vehicles; Epsi Minnows and RBR Concerto-based profiling vehicles; Profiling vehicle recovery team; Profiling vehicle on board

Shipboard CTD and Lowered ADCP

We conducted 8 CTD/LADCP profiles in the Jan Mayen channel, including profiles near both the acoustic source and receiver moorings. Profiles were concentrated on the southern slope of the channel, where previous work observed deep water transport. The LADCP was supplied and set up entirely by the ship crew, which we were appreciative of.

V-Wing

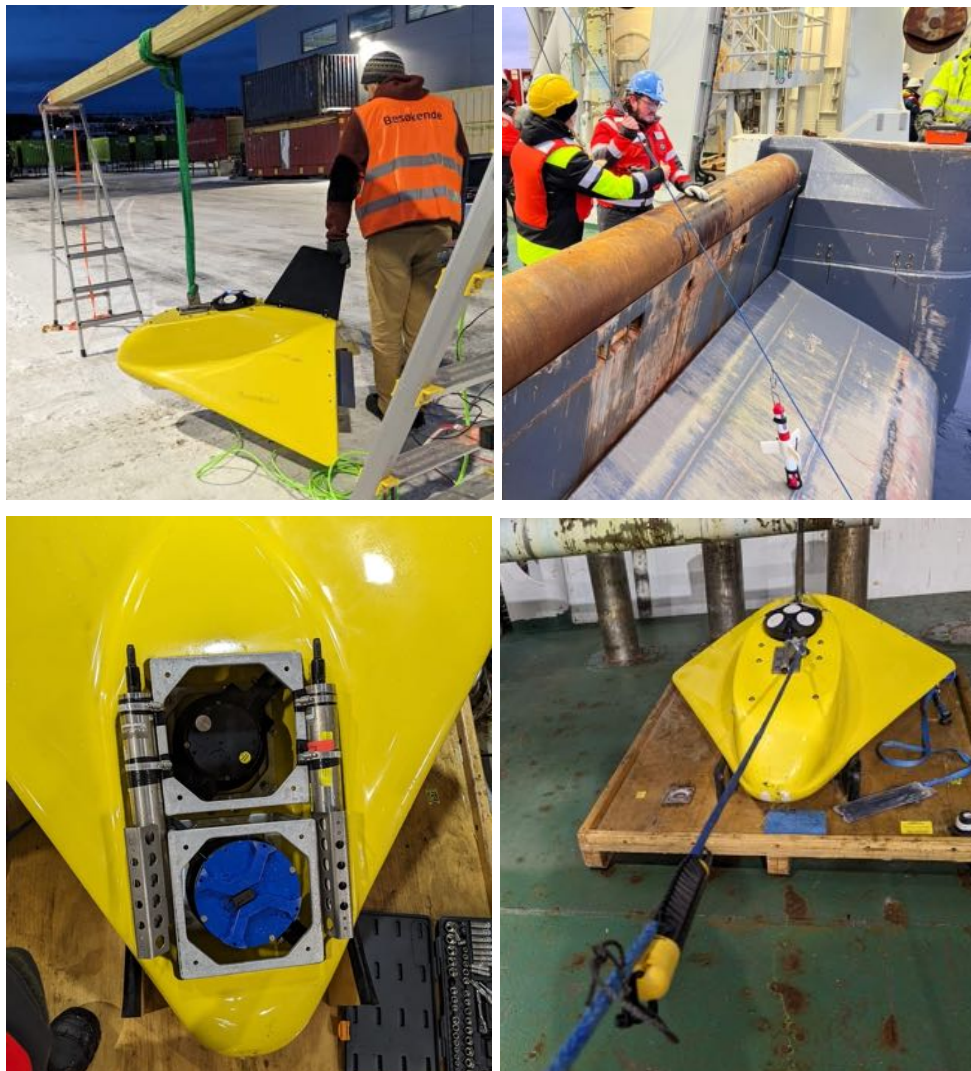


Figure 6: Clockwise from top-left: Compass calibration on shore; deployment of concerto attached to the line via bale hose clamped to instrument+carabiner through loops on line; underside of V-Wing showing mounting of SBE37s and ADCP casings (downward facing instrument not included but case included for extra weight); attachment technique for solo Ts and Duets

The V-wing is a tow-body with upward looking ADCP mounted inside. Additionally, instruments are attached along a 300m length of $\frac{3}{8}$ amsteel. Instruments are attached via carabiners to fixed loops in the amsteel line as the tow-body is deployed, and using zip ties and tape. More details of the deployments and procedure are given in the Appendix.

Bow Chain



Figure 7: Left: Deployment of the bow chain from the starboard side of the ship. The line of thermistors is lowered by the science crew as the 200lb weight is lowered by the winch and the ship's knuckle crane. Right: an example of the thermistor attached to the line. The line was 30m long with 59 thermistors attached every 0.5 m.

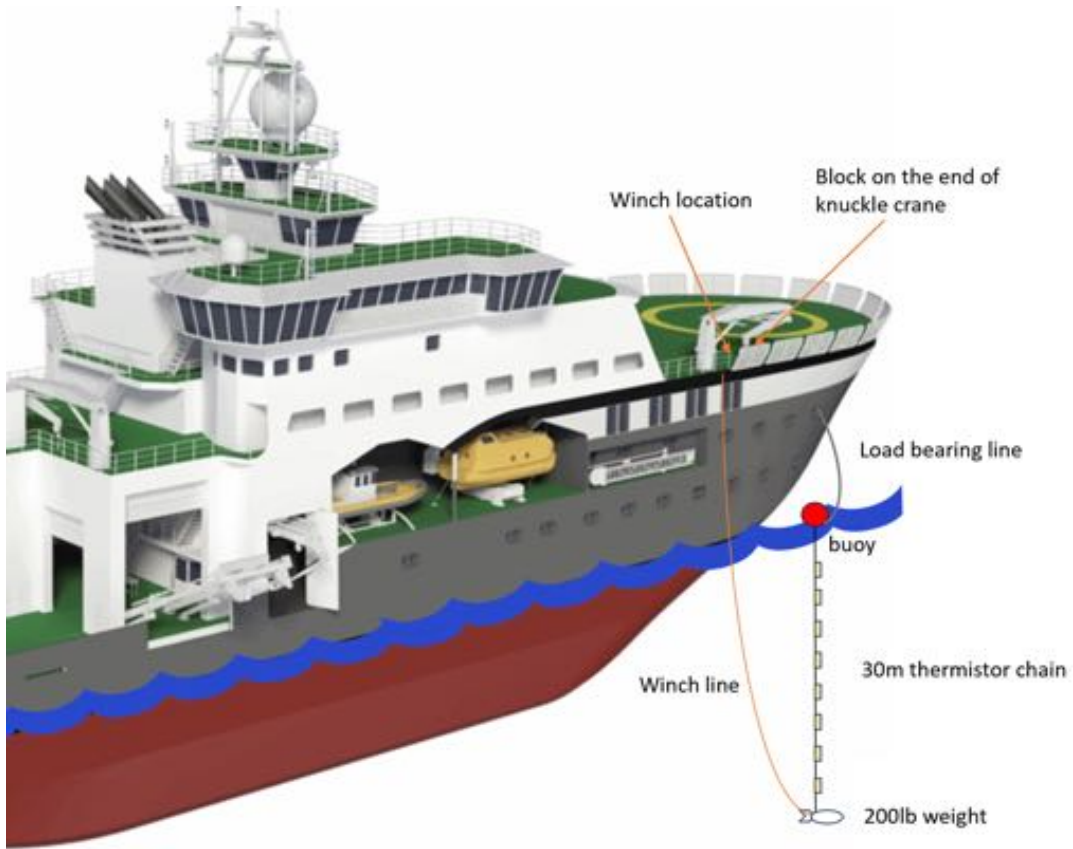


Figure 8: Schematic of bow chain deployment

The bow chain consists of a 30-m wire to which RBR soloT thermistor sensors are clamped (seen Figures 7-8), a 200lb weight, a load-bearing line, a winch line, and a buoy. For deployment, the weight is lowered using the winch line which is run through a block on the ship's knuckle crane. As the weight is lowered, the thermistor chain is let down, hand over hand. There is a slip line that runs through a pear link on the buoy that allows us to slowly lower the top of the thermistor chain and the buoy to the sea surface. The load bearing line is secured in the mooring line room, which is a deck below the helicopter pad, and runs through a hawsehole. The weight is lowered until the winch line goes slack and the load bearing line takes all of the tension for the duration of the deployment. The crane and winch line are then secured during deployment. The deployed chain had a total of 59 sensors, 5 RBR Duets to measure temperature and pressure, and 54 RBR solo thermistors. Bow chain deployments are listed in the appendix.

Gliders

Multiple types of gliders were deployed and recovered at different points in the cruise. The types of gliders and their missions are summarized in Table 2 below. The deployment and recovery procedures for

the various gliders depended on the type and weather conditions. All recovered gliders were left outside on deck for a minimum of 18 hours because of the battery precautions.

| <u>Glider Type</u> | <u>Deployment Plan</u> | <u>Sensors</u> |
|-----------------------|---|--|
| SeaExplorer "SEA064" | Around Jan Mayen, circumnavigation | turbulence/ADCP/CTD/DO |
| Slocum G3S "Electa" | Shuttle between source and receiver moorings, then follows DBASIS | CTD / FLBBCD / passive acoustics (HTI-96 hydrophone matched with Loggerhead LS1) |
| Slocum "Freya506" | pre IOP: shuttle between source and receiver moorings | turbulence/CTD |
| Slocum G3 883 ("Urd") | Large-scale survey around the Jan Mayen region | CTD |
| Seaglider "SG560" | Recovery in LBE; has been sampling in the eddy since 21 May 2023 | CTD, DO |
| Waveglider ("WG") | Transit from Iceland, then shuttle between moorings | Wind / pressure /rh/ a temp, directional surface waves, 300khz adcp |

Table 1: Gliders

Seaglider sg560 was recovered on the 9th of November 2023 in the Lofoten Basin Eddy (LBE) using the small boat. A crane was used to pull the glider from the small boat up on deck, where it was placed in its cradle and strapped down. This glider has been sampling CTD and DO in the upper 1000m of the LBE (spiraling in and out of the eddy) since 21st of May 2023.



Figure 9: UiB Seaglider sg560 recovery

Slocum G3 glider 883 (“Urd”) was deployed in the Jan Mayen Channel on 14 November 2023 from the starboard crane. Urd is rated to 1000-m depth and equipped with a pumped SBE CTD sensor. During the cruise, Urd occupied a section along the Jan Mayen Channel. Urd was supposed to remain deployed for several months, but because of bad conductivity readings (too high values compared to the other assets in the water, and an uncorrectable non-linear drift at depth), we decided to recover Urd at the end of the cruise (27 November 2023) and the SBE CTD will be shipped back to service. The glider was recovered by the starboard crane and using the nose release system on the glider. The temperature measurements taken along the Jan Mayen Channel look good and we see evidence of the subsurface temperature maxima in the entire channel.

The VIMS team operated two gliders during the cruise: VIMS SeaExplorer X2 SEA064 French Lady, equipped with CTD, DO, a Nortek AD2CP with realtime absolute velocity processing, and Rockland MicroRider with realtime turbulence processing; and VIMS Slocum G3S Electa equipped with CTD, FLBBCD, and passive acoustics. Laur Ferris, Donglai Gong, and Nicole Trenholm conducted functional checkout and calibrated the gliders’ flight and ADCP compasses at the warehouse during the mobilization period. The team located a site suitable for compass calibration by mapping the magnetic field of the warehouse and parking lot via hand compass. Ferris and Trenholm embarked on the cruise, and the gliders were deployed via aft starboard crane with a quick release hook. French Lady conducted a complete clockwise circumnavigation of the Jan Mayen in order to gain insight into the broader dynamics of the region away from the NORSE mooring site, and contextualize water masses influencing site of shipboard and Lagrangian sampling. Electa completed two transects between the ASM and PECOS moorings, diverted to follow the DBASIS buoy on November 18th when the moorings were recovered, and was sent south on November 20th to repeat French Lady’s southeastern transect of Jan Mayen

November 20th during the storm. The gliders were piloted by Jack Slater, Gong, Ferris, Trenholm, and Ricardo Bourdon, and recovered on November 27th via small boat, with Ferris on the boat and Trenholm receiving the vehicles on deck.

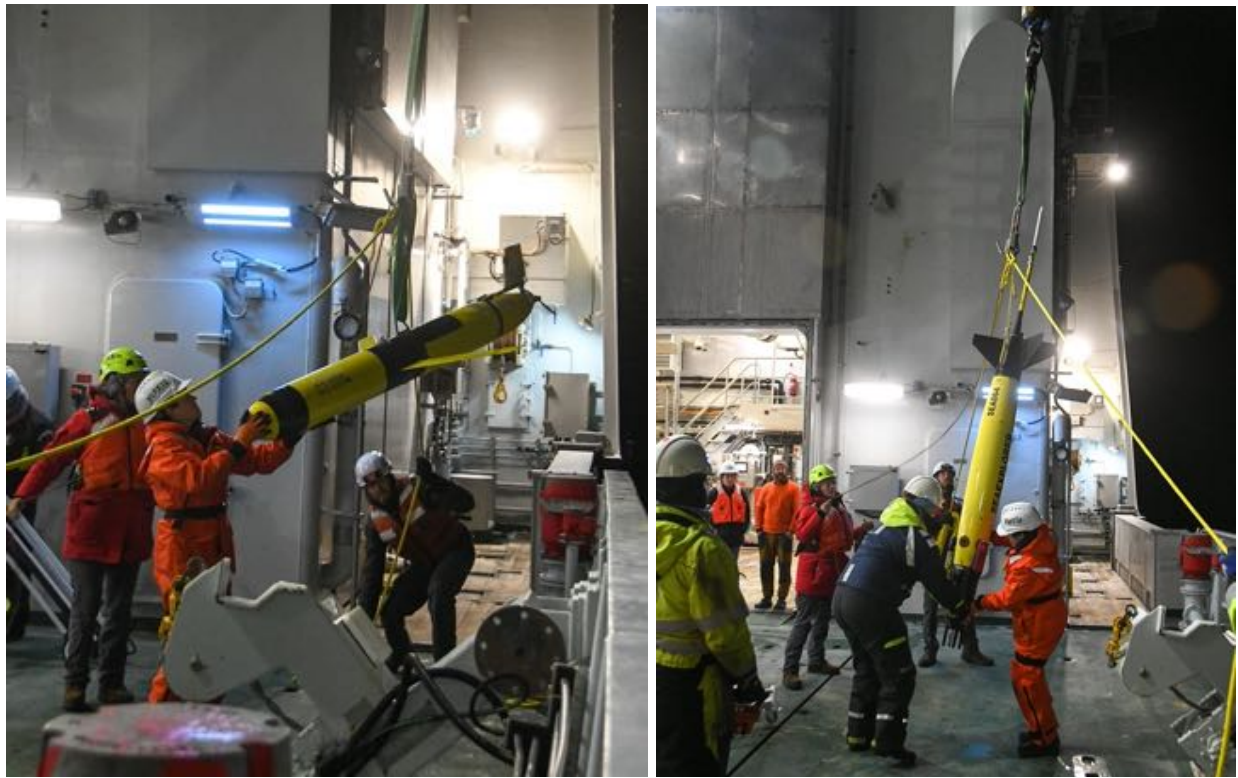


Figure 10: Slocum and SeaExplorer glider deployments (photos by Kerstin Bergentz)

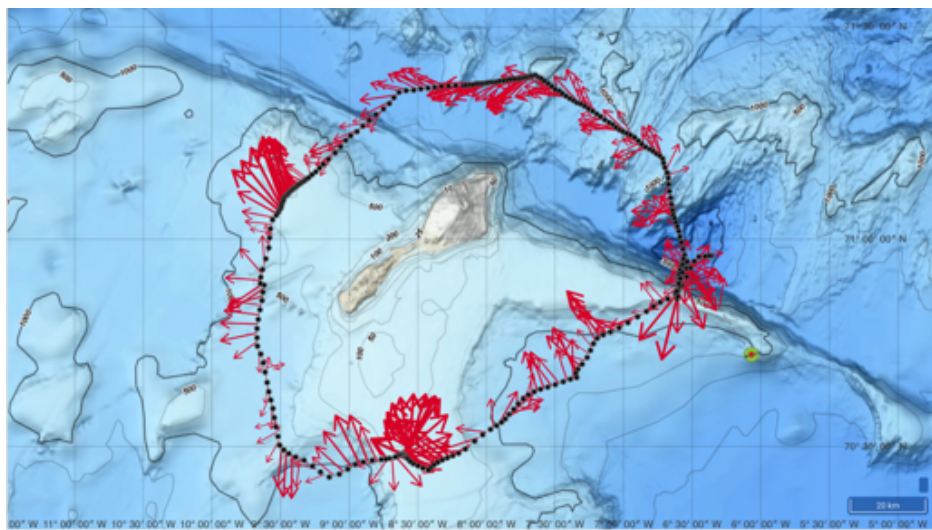




Figure 11: Maps showing mission trajectories for SeaExplorer French Lady (top) and Electa (bottom)

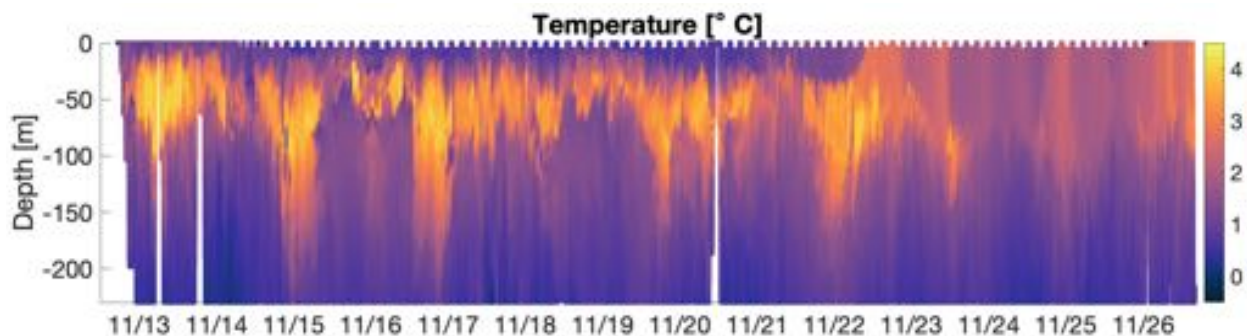


Figure 12: Recovered temperature observations from Slocum Electa, focusing on the upper 200m. Showing rapid surface evolution on 21-26 November

Floats and Drifters

Surface Drifters and ALTO floats (non-recovered)

A total of 12 SVP drifters, 2 MiniMets and 2 DWSD (directional wave spectra drifters) were deployed in the Lofoten Basin Eddy on the evening of November 9th local time. In addition multiple sets of drifters were deployed around the Jan Mayen area to help provide context for the acoustic experiments. First there were 4 SVPs deployed during the initial ADCP survey next to Jan Mayen overnight 12-13th of November. 2 MiniMets and 4 DWSB were deployed in an array with acoustic instruments on November 15. The last two DSWB were used to reseed the acoustic array on November 20th. All the above mentioned drifters were deployed from starboard aft deck. More information on each type of drifter can be found at <https://gdp.ucsd.edu/ldl/>.

4 ALTO floats were deployed together with the drifters in the Lofoten Basin from the same location on the ship but with a crane and quick release sprint.

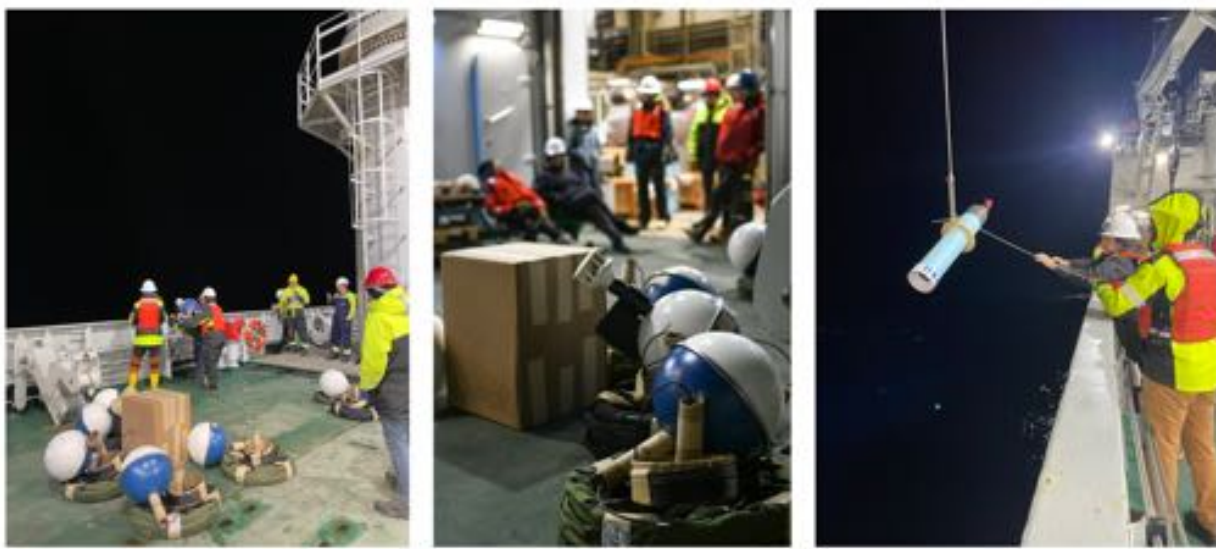


Figure 13: Drifter and ALTO deployments on November 9th

Hydrophone Drifters (recovered)

In total, 5 CMRE SVP drifters with hydrophones at 20, 30 and 40 m, 2 SIO MINIMET drifters with 1 hydrophone, 6 SIO DWSB drifters, 2 standard SIO MINIMET drifters, and 4 APL SWIFT V3 drifters with hanging hydrophone were deployed during the acoustic experiments on 15 and 20 Nov (pre-storm) and 15 Nov (post-storm) in the JM area.



Figure 14: Deployment of a CMRE SVP drifter: surface buoy (blue-white-orange), drogue (blue) and hydrophone array (orange/black cables and black hydrophones and pressure-temperature sensors).

The 2 SIO MINIMET drifters with hydrophone stopped transmitting on 17 Nov and were recovered. The CMRE SVP drifters were recovered on 20, 25 and 26 Nov. Recoveries were done with the small boat.

Acoustic Profiling float (recovered)

We conducted 2 deployments of the CMRE profiling float fitted with a compact 3D acoustic array. This is a PROVOR Argo float modified to add the acoustic payload. Deployments and recoveries were done with a small boat. The first deployment on 13 Nov had a short mission period of 6 h to test the diving capabilities of the float. The float was then redeployed on 15 Nov and recovered 5 days later. It performed 21 dives down to 150-300 m, collected CTD data on the descent and directional acoustic data continuously.



Figure 15: The CMRE acoustic float being deployed with the crane off the starboard side .

SWIFT Drifters

The primary purpose of SWIFT drifters is to measure surface wave displacements to compute directional wave spectra, and to measure vertical profiles of turbulent kinetic energy dissipation rate in a surface following reference frame. SWIFTS also measure near-surface wind speed and air temperature, as well as sea temperature and salinity and so can be used to compute surface fluxes. A total of 11 SWIFT (Surface Wave Instrument Floats with Tracking) drifters were deployed and recovered throughout the cruise, for a cumulative 20 individual deployments. A full list of deployment times and locations is provided in the Appendix. Of the twelve available SWIFTS, eight were version 4 (shorter, equipped with Nortek Signature1000 down-looking ADCPs to measure turbulence) and four were version 3 (taller, with hydrophones hanging below on a 15m elastic line). SWIFTS were deployed in proximity to other assets, predominantly the DBASIS buoy, as well as around surface features of interest. The primary goal was to obtain continuous time series across a wide range of surface conditions, so great effort was taken to

ensure SWIFTs were continually in the water between the first and last deployments. When possible, efforts were made to pair V3 and V4 SWIFTs with the goal of comparing uplooking (0-1m) and downlooking (1-5 m) dissipation rate profiles from the two versions. SWIFT positions and on-board processed burst-averaged data were telemetered via an Iridium modem.

Version 4 SWIFTs were deployed over the side on a slip line. Version 3 SWIFTs were deployed with a crane, with the hydrophone lowered over the side. Both versions were recovered using a grappling line and boat hooks to pull the instrument aboard by hand. Deployments and recoveries were uneventful with the exception of SWIFT 15, which was missing its hydrophone upon recovery from its final deployment during the storm. The elastic line was cut ~1m from the base of the drifter. This may have occurred during deployment or recovery when the drifter was dragged alongside and under the vessel. Data from the earlier acoustic experiments had already been recovered, so only data from the storm period was lost.



Figure 16: version 4 (left) and version 3 (right) SWIFT buoys. The v3 buoys include a small heave plate and hydrophone hanging 15 m below the buoy.

Sound source from the ship

A NEPTUNE D/11/BB source was operated from the ship during the three intensive acoustics experimental periods on 15, 20 and 25 Nov. It is compact (< 26 cm) and lightweight (7.7 kg). It was connected to an acoustic rack (with power amplifier, signal generator and GPS antenna) in the laboratory with a cable. Sound transmissions were turned on 5 times for about 10 min at locations separated by 2 or 3 nm, near the drifters with hydrophones and the DBASIS buoy. The target source depth was 20 m, but due to strong winds the cable was inclined and the actual source depth varied between 10 and 20 m. The sound signal consisted of 4-s up-sweeps between 8 and 15 kHz, transmitted every 10 s. The source level was 184 dB re 1 μ Pa/V @ 1 m.



Figure 17: The Neptune D/11/BB source waiting to be lowered on the aft deck, starboard side, between periods of sound transmission.

5. Preliminary Results

Overview

The ocean we encountered in 2023 was distinct in several ways from that of previous NORSE cruises. The most dramatic difference was the presence of a sub-surface heat maximum in the Jan Mayen region. Profiling and glider measurements revealed an energetic ‘soup’ of submesoscale eddies between the warm salty Atlantic water to the east and the cool fresh polar water to the west. Within this transition zone, warm Atlantic water with a particular T-S value was found between 50 and 100 m depth, overlain by cooler fresher water that appeared to be formed by lateral stirring and mixing of the eastern and western water mass endpoints. The warm subsurface layer was far from uniform, but instead appeared in the form of sub-surface vortices, blobs, and filaments with horizontal scales of order 10 km and less.

The presence of this subsurface heat maxima created a unique acoustic duct, one with order 50 meter vertical scale but with significant horizontal patchiness. Exploration of the consequences for transmission, scattering and loss of this submesoscale acoustic duct was a major goal of our sampling this past month. We are hopeful this integrated PO/Acoustics dataset will provide a novel look at upper ocean sound propagation in the presence of an energetic submesoscale field.

The other major difference from the 2022 work was the arrival of a strong storm mid-way through the cruise. Though the ship itself ceased profiling work during the peak (70+ knot) winds and (~8 m) waves, DBASIS, gliders and drifters provided a fantastic time series of the build up and recovery from a well defined strong surface forcing event. Following the storm, ship and glider profiling revealed that the

subsurface heat maxima was still present, though the upper portion had been eroded by mixed-layer deepening (with its heat presumably released to the atmosphere). Even in the 1-2 days we sampled after the storm, the ocean was already beginning to slump and laterally re-stratify.

Finally, glider, wave-glider and CTD/LADCP measurements helped place this work in a regional context, showing the relationship between both different water masses in adjoining basins and the deeper water mass transport below our focus depth range. In the subsections below we explore these results in more detail.

Meteorological conditions

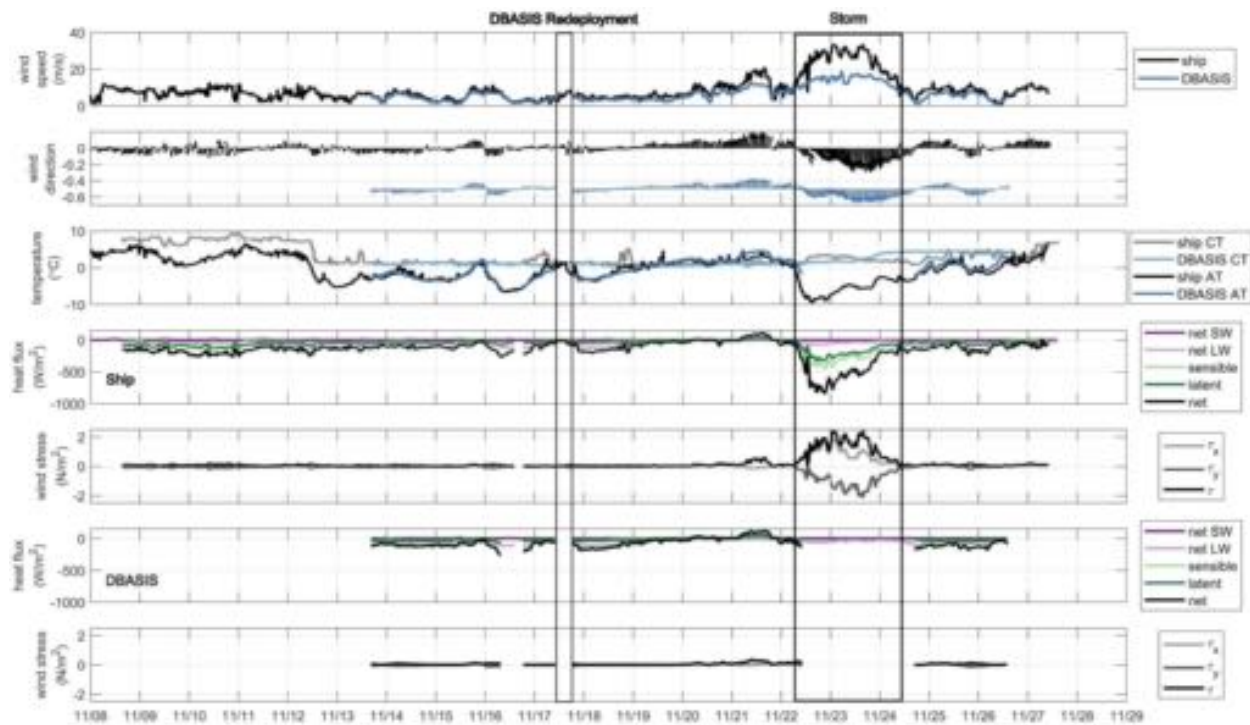


Figure 18: Wind speed, atmospheric temperature, and sea surface temperature recorded by shipboard instruments and DBASIS. Heat flux (net shortwave, net longwave, sensible, latent and net) and wind stress computed with the COARE 5 bulk flux algorithm without the wave parameterization. Positive (negative) heat flux indicates heat transport into (out of) the ocean. Shortwave and longwave radiation were not available for the ship and fluxes were computed with DBASIS measurements, assuming low regional variability.

Before and after the storm, winds are approximately 4 - 6m/s. The atmosphere is generally cooler (-3°C) than the ocean (1.5°C) but there are a few periods when atmospheric temperatures approach sea surface temperature. These co-occur with winds from the south. Heat fluxes indicate a net cooling of the ocean ($\sim 200 \text{ W/m}^2$) except for a brief period before the storm.

During the storm (Nov 22 to Nov 24, 2023), winds recorded by DBASIS increased to 16m/s and even higher values were observed on shipboard instruments (30 m/s). Winds were predominantly from the north. Atmospheric temperature recorded by the ship dropped to -8°C and net heat flux out of the

ocean was $\sim 800\text{W/m}^2$. Atmospheric temperature sensors on the DBASIS froze during the storm so heat fluxes could not be computed. Comparisons with other instruments or ERA reanalysis will be made at a future date.

Stirring and subduction, spice and subsurface heat maxima near Jan Mayen

A composite Satellite Sea Surface Temperature (SST) (Fig. 19) clearly shows the warm Atlantic water on the Easterns side of our study region, the cool polar water on the Western side, and a transition zone in between. Most of the ship-board profiling took place where surface water was cool (dotted transect lines in Figure 19), but the sub-surface structure was a panoply of subduction, stirring and mixing.

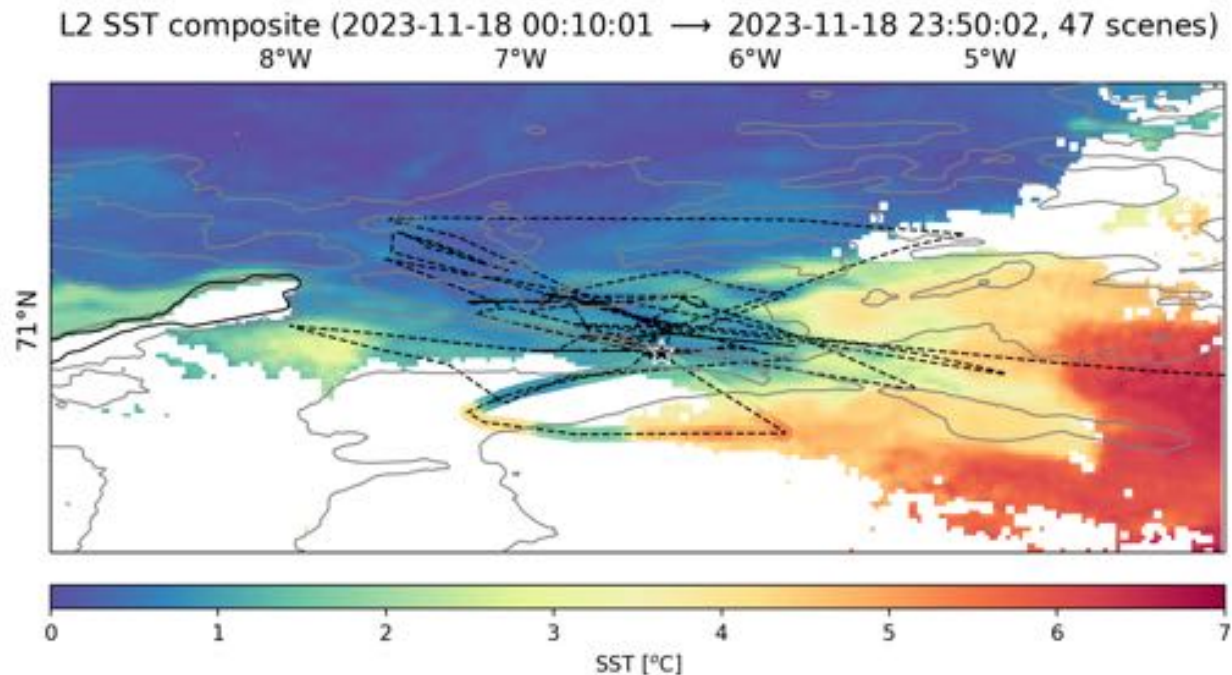


Figure 19. SST composite gridded from 47 scenes from six different satellites (24 h composite to mitigate patchiness due to cloud cover), around the time of one of the cross-front profiling transects. The ship flow-through temperature during the time of the composite is overlaid on the same color scale. The ship track is the dashed black line. The black star indicates the ship's position at the end of the SST composite period. The gray lines are the 100, 1000, 2000, and 4000 m isobaths.

Ship-board profiling in the transition region reveals a strong sub-surface heat maximum (Figure 20), consisting of warm salty waters underneath colder fresher waters. The subsurface heat anomaly is patchy, ranging in vertical extent from almost 100 m to only tens of meters, over lateral scales of 1-10s of km. (Figures 20, 22). Currents in this region show a strong internal tide signature (see subsection below) with a mode-one characteristic vertical scale. To highlight the submesoscale currents in the upper

ocean, in Figure 20 we plot the currents averaged in the upper 50 meters minus the currents averaged from 150-250m - this roughly removes the internal tide signature. Currents plotted this way (black arrows in Figure 20) show a complicated sea of submesoscale eddies, with similar horizontal scales as the sub-surface temperature structures.

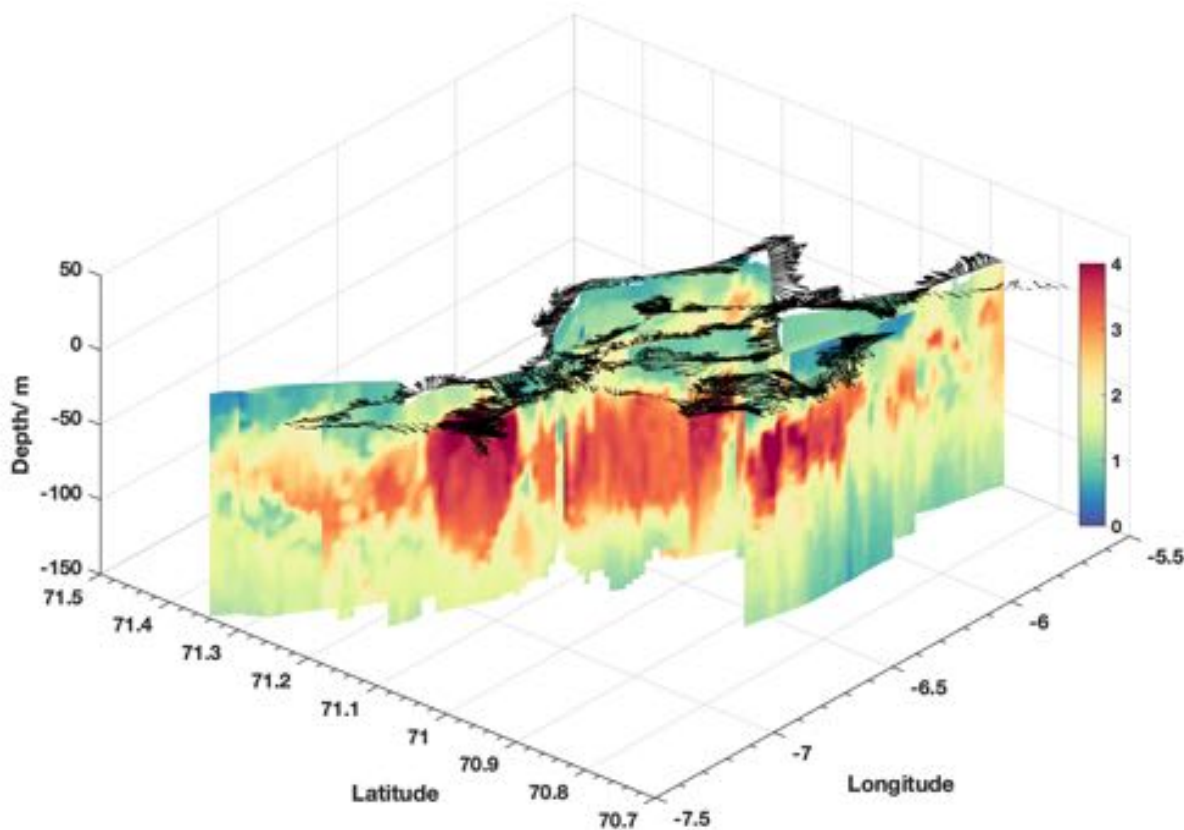


Figure 20 - Temperature (before the storm) as measured by the profiling CTD and Epsi. Vectors show the current anomaly in the top 50 meters (with the average currents between 150-250m subtracted out).

The warm salty sub-surface water mass shows up clearly in Temperature-Salinity plots as a maximum in a water mass histogram (Figure 21). The overall histogram reveals a complicated interplay of stirring and mixing between warm salty Atlantic Water (upper peak), cool fresh polar water (lower left end-point), and the intermediate and deep water that is found on both sides of the ridge (bottom right). The contour near the upper right peak is what we use to identify this water mass for subsequent analysis.

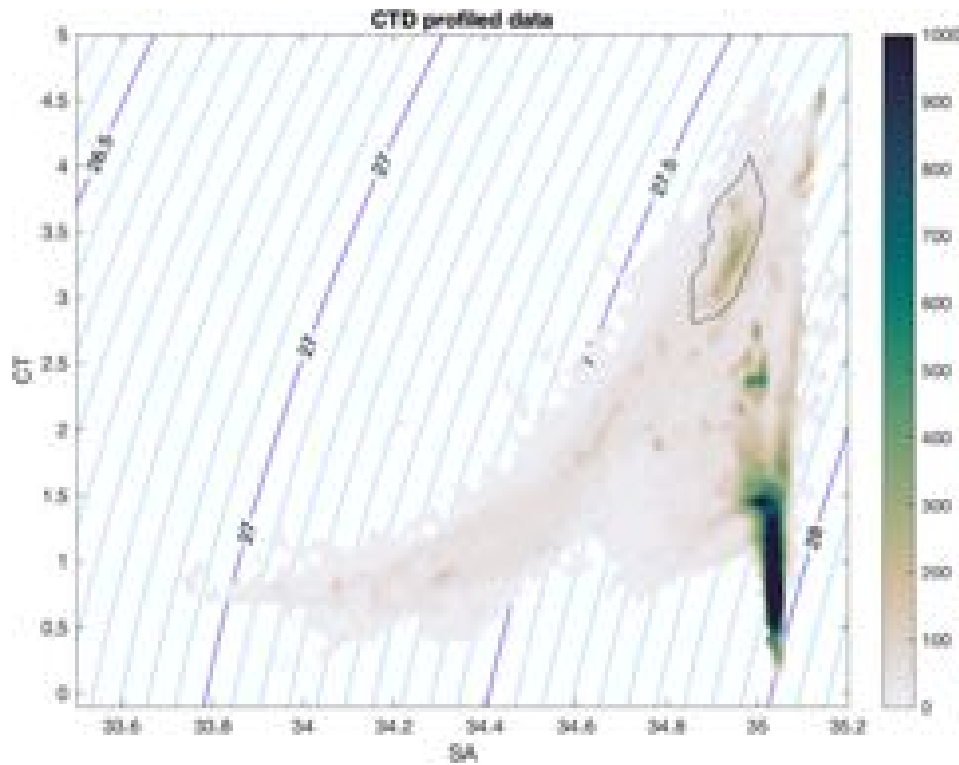


Figure 21: Temperature and Salinity histogram from CTD and Epsi throughout the entire survey. The black circle encompasses the T-S properties of the warm subsurface water mass observed consistently before the storm.

Identifying the warm water mass using a threshold of 3°C allows us to characterize its structure. The warm mass bounded by those isotherms gets both deeper and thinner towards the Northwest portion of the study region (Fig 22), suggesting that subduction may have occurred in the Southeastern portion of the study region. This water mass class was also observed in the surface in a narrow density range on the Southeastern side of the survey area.

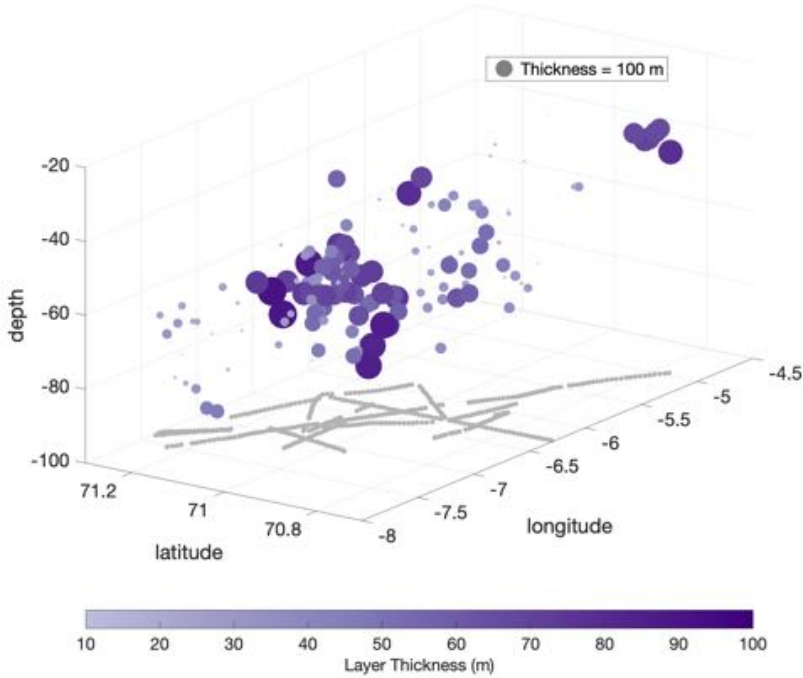


Fig 22. The thickness of the warm layer is represented in both size and color of the circles at a specific location. The depth of the circles represent the mean depth of the warm water mass. Generally, the warm waters get deeper towards the northwest.

The CMRE profiling float and the DBASIS buoy both provided semi-Lagrangian measurements of the upper water column structure as they slowly drifted through the region. After an initial test dive on 13 Nov, the CMRE float was redeployed on 15 Nov and performed 21 dives until its recovery on 20 Nov. The target parking depth was 250 m with varying sensibility range (up to 50 m). The float technical parameters were continuously trimmed optimize the dive characteristics. The cycle length was initial set to 6 h. Starting at cycle 12, it was changed to 8 h to increase the time at parking depth, and then decreased to 6 h at cycle 24, when the technical parameters were optimized and kept constant. Practically, the cycle length varied between \sim 4.5 h and \sim 8 h, and the maximum diving depth between 150 and 320 m.

CTD data from the CMRE float were acquired on the up cast for the first two cycles. For cycles 3 to 21, the CTD was turned off during ascent in order to reduce self-noise, and was turned on during descent. In this way, during ascent there is practically no self-noise since the CTD pump is off and there are no hydraulic pump or valve actions. Below about 200 m, the sampling period was 1 h, since the float considered to be at parking depth. During ascent and descent, it was 1 Hz.

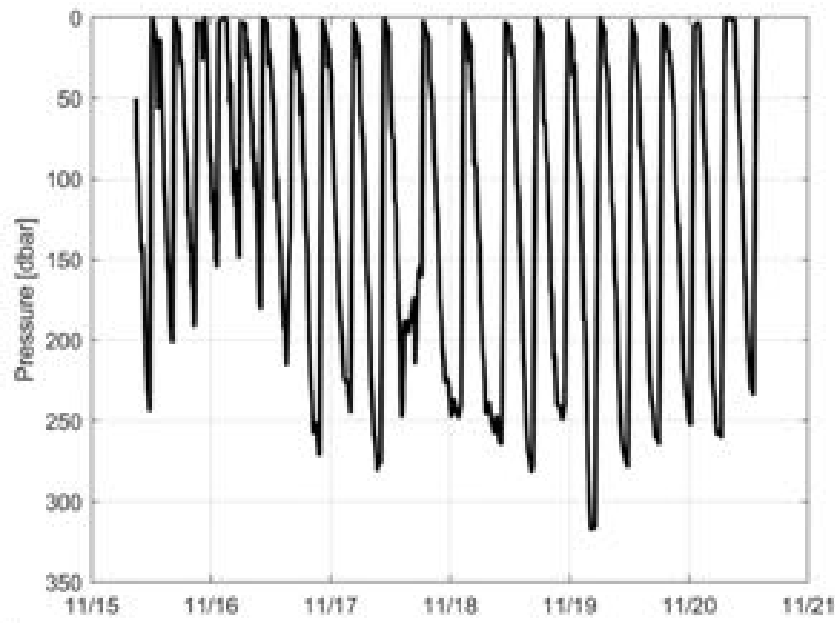


Figure 23: Pressure versus time for float cycles 1 to 21, between 15 and 20 November 2023.

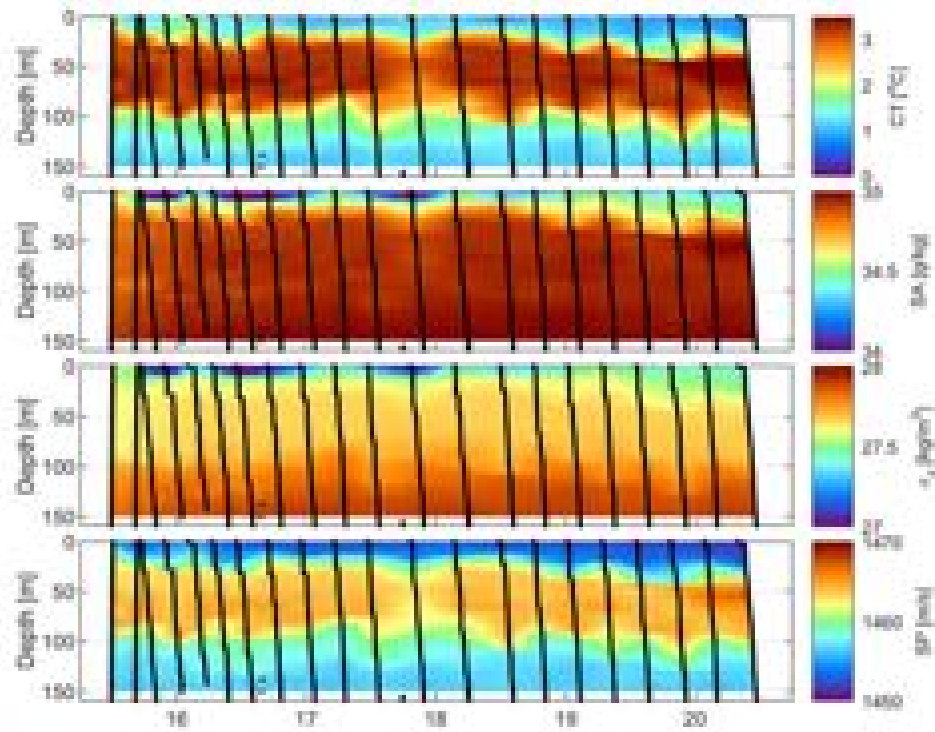


Figure 24: Interpolated and color-coded conservative temperature (CT), absolute salinity (SA), potential density anomaly (σ_0) and sound speed (SP) versus time and pressure (depth) as measured by the float CTD between 15 and 20 November 2023 (cycles 1 to 21). The location of the data in time and depth are shown in black.

The profiling Wirewalkers on the DBASIS buoy also slowly drift through the warm subsurface structure, showing a rich array of detail (Figure 25). An intricate series of shear layers bound the sub-surface heat maximum, both above and below.

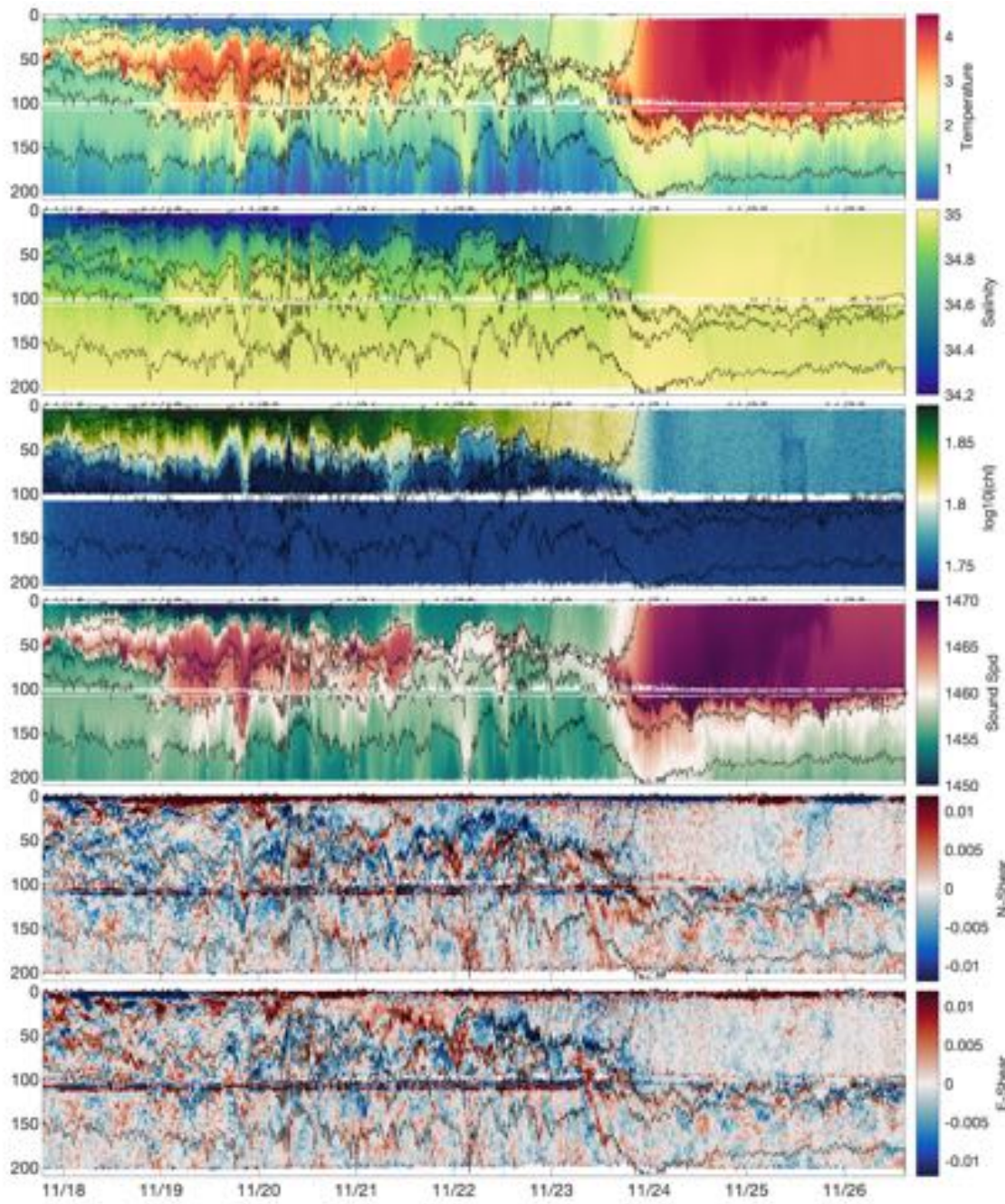


Figure 25. Wirewalker time series of water column properties, chlorophyll, calculated sound speed, and the two components of velocity shear. The strong storm took place between Nov 23-24.

Acoustics: submesoscale upper ocean structure around Jan Mayen

We conducted a series of joint acoustic-oceanographic experiments using a ship deployed source and recording the signals on hydrophone-bearing SVP drifters and hydrophones. For each experiment, the drifters were positioned along a 10 nm transect. The source transmissions were broadcast from five stations equally spaced over the transect. The signal was a repeated sequence of four-second-long chirps in the 11 kHz to 15 kHz frequency band. At each station, the signals were broadcast for ten minutes while the ship drifted. The source depth was 20 m and the receiver depths were between 10 and 40 meters. After the acoustic measurements were completed, the water column properties were sampled using the shipboard profiling system. The measurements for the first two experiments were collected with the Concerto CTD, and the measurements for the third experiment were collected with the Epsi fish.

An example of spectrogram for the deepest hydrophone attached to one of the drifters (near 40 m depth) is shown in Figure 26 below. The signal emitted by the NEPTUNE source is seen as a main and one subsequent secondary 4-second-long LFM upsweeps between 8 and 15 kHz, corresponding to direct and reflected paths, respectively. There is a delay of ~ 1.13 s between the direct signal and the reflected one, corresponding to a distance of about 850 m. The LFM upsweeps of the WHOI source installed on the DBASIS buoy appear between 610 and 890 Hz.

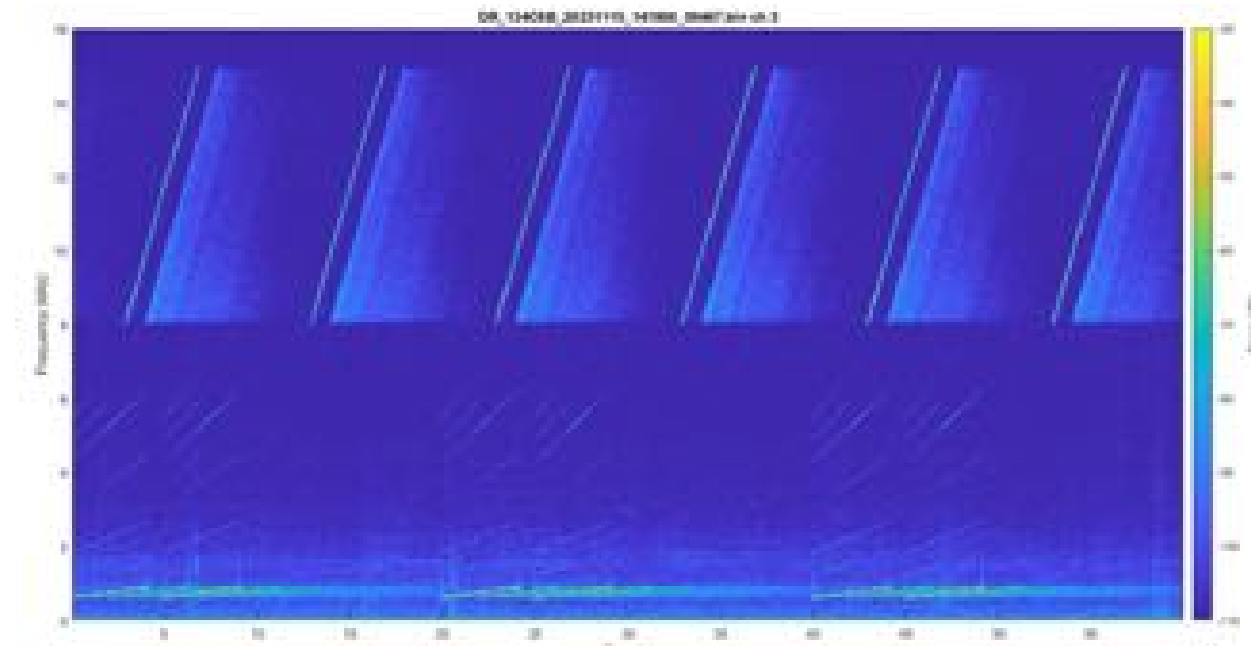


Figure 26: Spectrogram of the deeper hydrophone for CMRE drifter 64302450, starting at 14:19 UTC on 15 November 2023.

A composite of multiple measurements from the three acoustics intensive experiments are shown in Figure 27 below. The first experiment involved the largest number of drifters, and they all show a general

trend of increasing transmission loss with increasing range. One notable exception is the receptions from station 5 which generally fall beneath the level observed from the other stations. At station 5, the source was in the subsurface temperature maximum instead of the acoustic duct, so that sound was not well trapped. For the second experiment, only one drifter was positioned along the source transect, but two SWIFTS were nearby and recorded the signals. Similar to the first experiment, at station five, the source is located in the subsurface temperature maximum and higher transmission loss is observed. The third experiment showed different characteristics both in terms of the water column properties and the acoustic propagation. The subsurface temperature maximum from the previous experiments is largely absent, and there is significant range dependence. The received level of the acoustic measurements shows more erratic patterns, and the received level is below the noise level for several of the stations. The reasons for these differences are the absence of the acoustic duct and the range variability of the ocean properties.

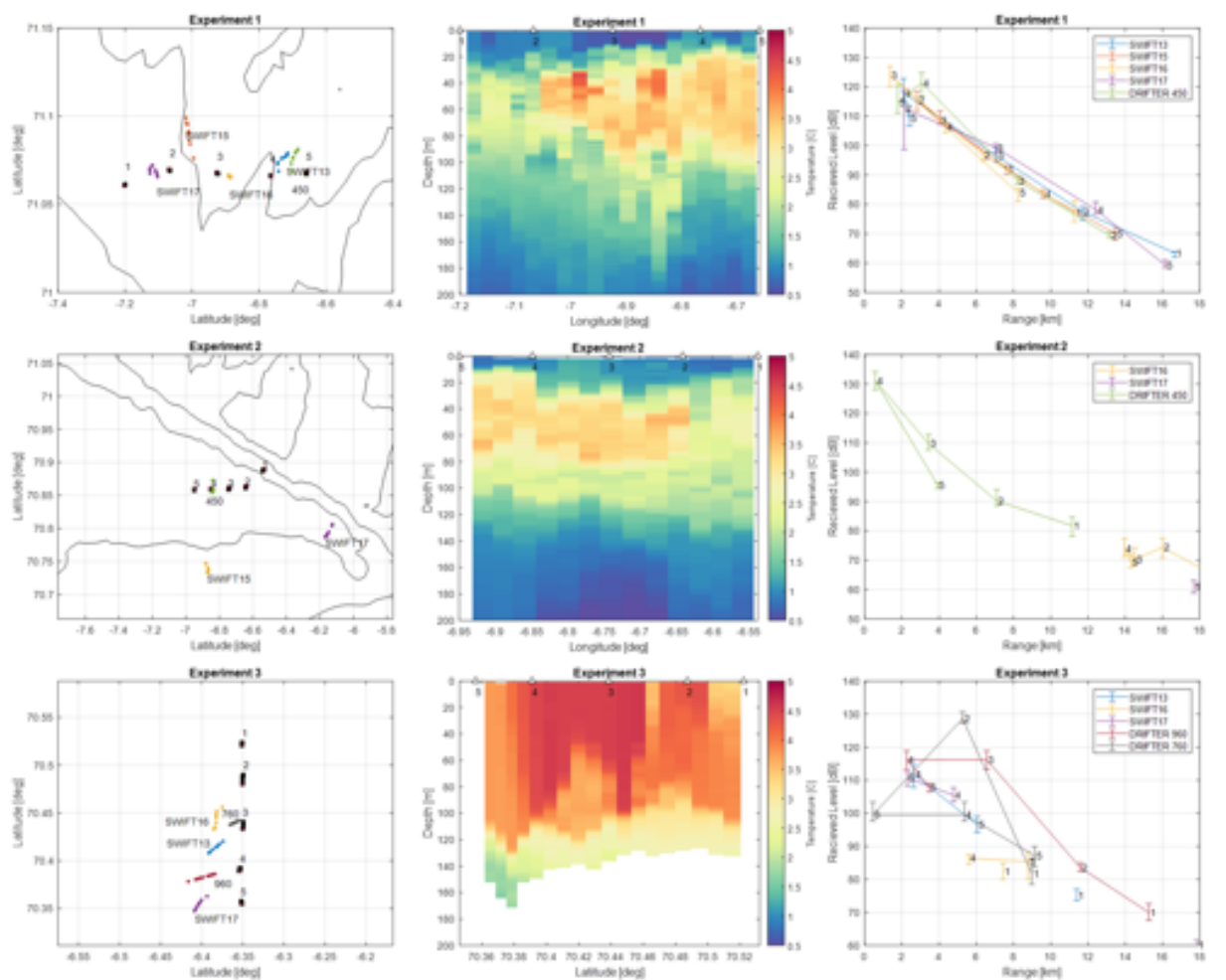


Figure 27: Summary of the series of experiments using the ship deployed source to broadcast signals to the hydrophones on the SVP drifters and SWIFTS. The first experiment took place on 15 November (top row), the second experiment took place on 20 November (middle row), and the last experiment took place on 25 November (bottom row). The left panels show the locations of the ship stations used to broadcast the signals (dark squares with numbered stations 1 through 5) and the locations of the SVP drifters and SWIFTS (colored dots). The center panels

show seawater temperature measured by the ship profiling system with the ships stations (white triangles and numbers). The left panel shows the received level of the mean of six pulse compressed signals with error bars representing the range of the measurements. The data are plotted as a function of distance from the source, and the source station for each set of receptions is indicated (some stations are missing because the signals could not be detected).

Strong Surface Forcing and SWIFT Wind/Wave measurements

On 23 November a strong low pressure system passed through the observational region (Figure 18). Initially we experienced moderate Southerly winds bringing warm moist air. Then after the low passed through we experienced a day of very strong Northerly winds, bringing cold air and snow. The ship itself sheltered behind Jan Mayen, where waves were low due to the limited fetch, but a down-slope effect in the lee of the Jan Mayen volcano led to ship-observed wind speeds topping 80 knots.

During the storm the SWIFTS had an excellent opportunity to measure the build up and decay of surface waves. SWIFTS sampled continuously for approximately 2 weeks in the vicinity of Jan Mayen, measuring surface wave spectra, wind speed and air temperature, ocean temperature, salinity and near-surface velocities and turbulence. Preliminary (burst-averaged) data were telemetered via satellite every hour throughout the deployment period. Figure 28 summarizes the atmospheric and surface conditions during the observation period from SWIFT telemetry data. Shown in the left column are near-surface wind speed, significant wave height, air and sea temperature, meridional drift velocity. Trajectories are plotted to the right. Onboard quality control sometimes prevented telemetry transmission of wind speed and wave heights, and we expect a good portion of missing data is likely to be recovered from post-processing the raw data, which will also reduce noise in the burst-averaged values.

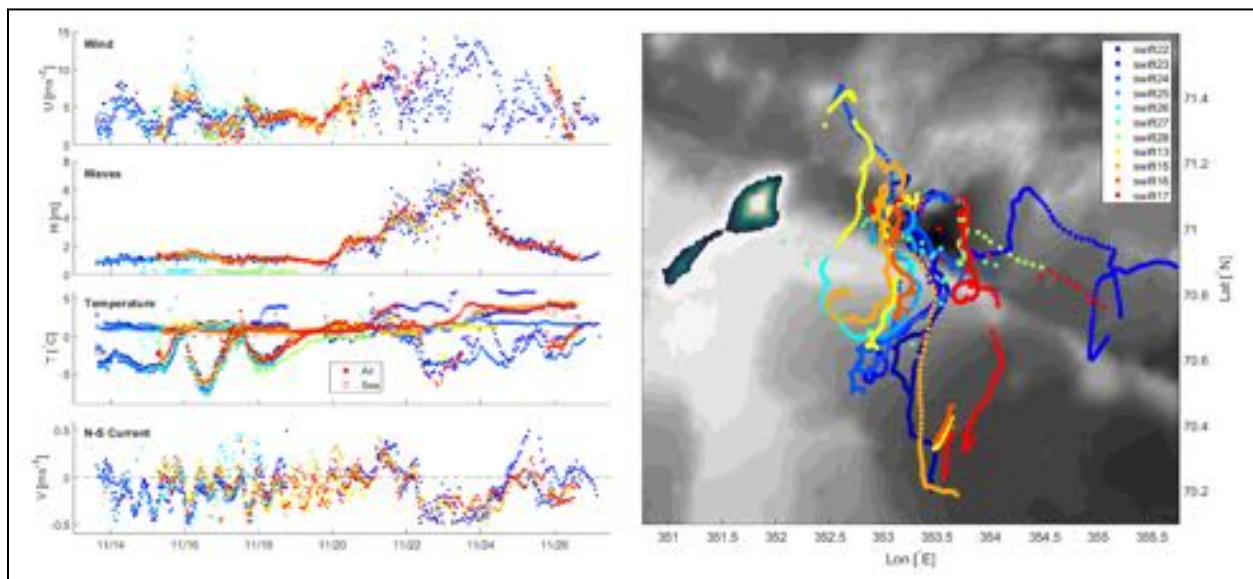


Figure 28. (Left) Near-surface wind speed, significant wave height, air and sea temperature and meridional drift velocity measured by all SWIFT drifters. (right) SWIFT drifter trajectories in relation to Jan Mayen. Note that SWIFTS

measured wind speed at 1 m (V3) and 0.4 m (V4) height. We expect post processing to reduce noise in the wave estimates and recover some missing wind speed measurements during the storm.

The observation period spanned two distinct regimes: a calm period with moderate wind speeds and minimal waves, followed by the storm beginning Nov 20. Wind speeds were often below 5 m/s prior to the storm, except for two moderate events with speeds up to 10 m/s. Note that SWIFTs measure wind speed at 1 m (V3) and 0.4 m (V4) height. These early wind events did not have a significant wave height signature, but brought cold air into the region and so likely had a significant impact on surface heat fluxes. During the calm period, SWIFT trajectories were dominated by inertial oscillations but were advected slowly southward on average. Wind speeds began increasing on Nov 20 as the storm arrived. Winds were highly variable but peaked around 15 m/s on Nov 24. The onset of storm winds on Nov 20 was accompanied by an abrupt increase in wave heights, from less than 1 m to 3 m within a few hours. From this point, wave heights increased gradually and reached 8 m under peak winds on Nov 24. As storm winds waned, wave heights decreased rapidly. This implies a significant difference between the character of surface conditions under the same wind speeds, i.e. as the storm built vs. subsided. This hysteresis will be an avenue of investigation. SWIFTs were swept southward during the storm, and frontal crossings can be seen in rapid changes in sea temperatures of a few degrees. Spatial variability in surface conditions under similar wind forcing will be another avenue of investigation.

Full wave spectra over the observation period emphasize the hysteresis in surface conditions described above. Shown in Figure 30 are burst averaged wave spectra from six SWIFTs with the greatest endurance during the observation period. As was apparent in time series of wind speed and significant wave height, storm and calm conditions are more sharply delineated by the waves than wind speeds. At all times spectra are dominated by waves with periods of a few to ten seconds. However, local wave growth spurred by changes in wind speed are apparent at higher frequencies. For example, a weak wind-sea peak at 0.5 Hz appeared on Nov 16 when wind speeds grew from near zero to 5 m/s within a few hours. The high-frequency peak moved to lower frequencies as the sea-state matured. Energy increased rapidly in all bands on Nov 20 as storm winds built, again with weak high-frequency wind-sea peaks which rapidly converged with the dominant wave band.

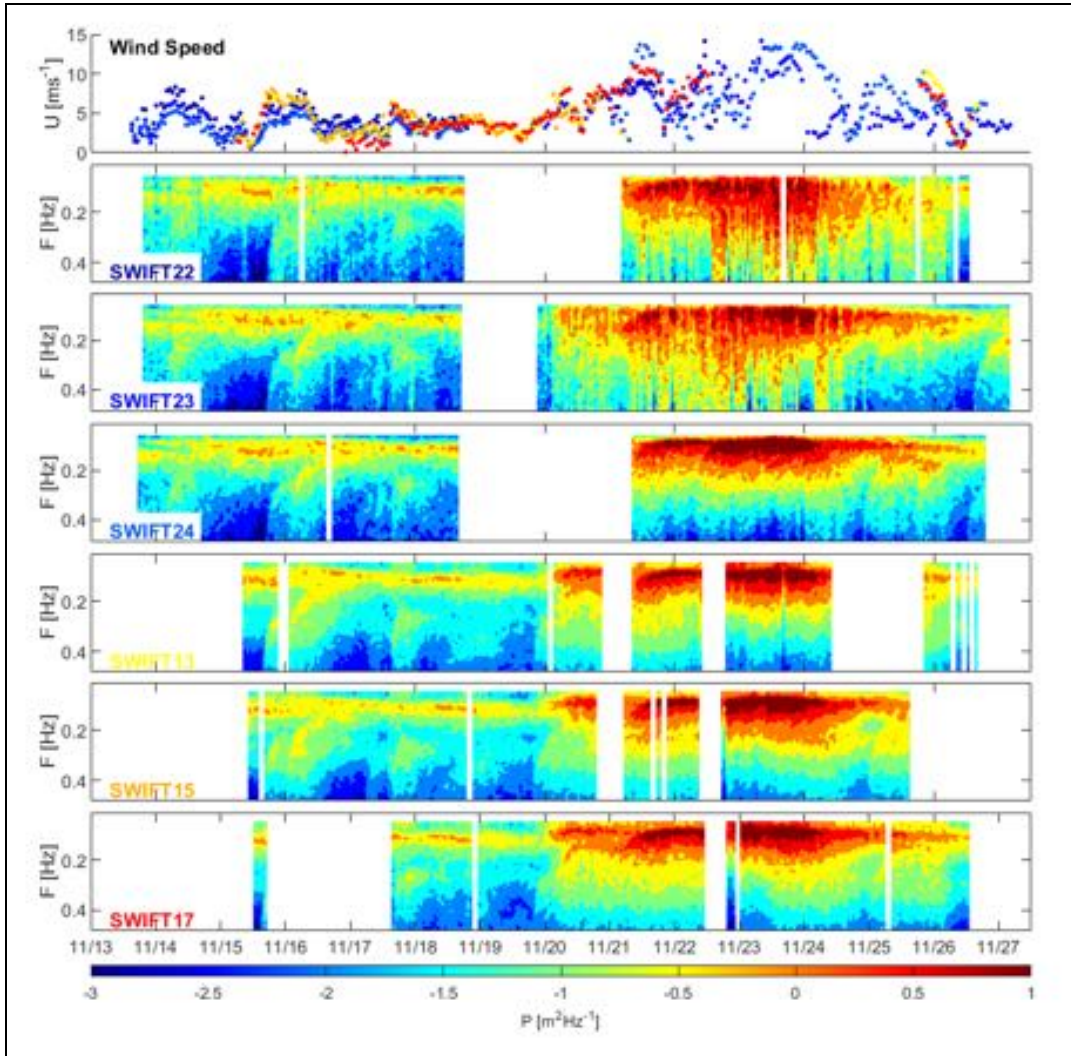


Figure 29. Full surface wave spectra from six of the SWIFT drifters, three each of V3 and V4. SWIFTs 22 and 23 are suspected to have had GPS dropouts leading to occasional spurious high wave power during the storm. These can be corrected in post-processing. Spectra are dominated by waves with periods of a few to 10s of seconds, but changes in wind speed generate wind-sea peaks at high-frequencies which grow in period as the wave field matures. Wind speeds from all SWIFTs are plotted at the top for context.

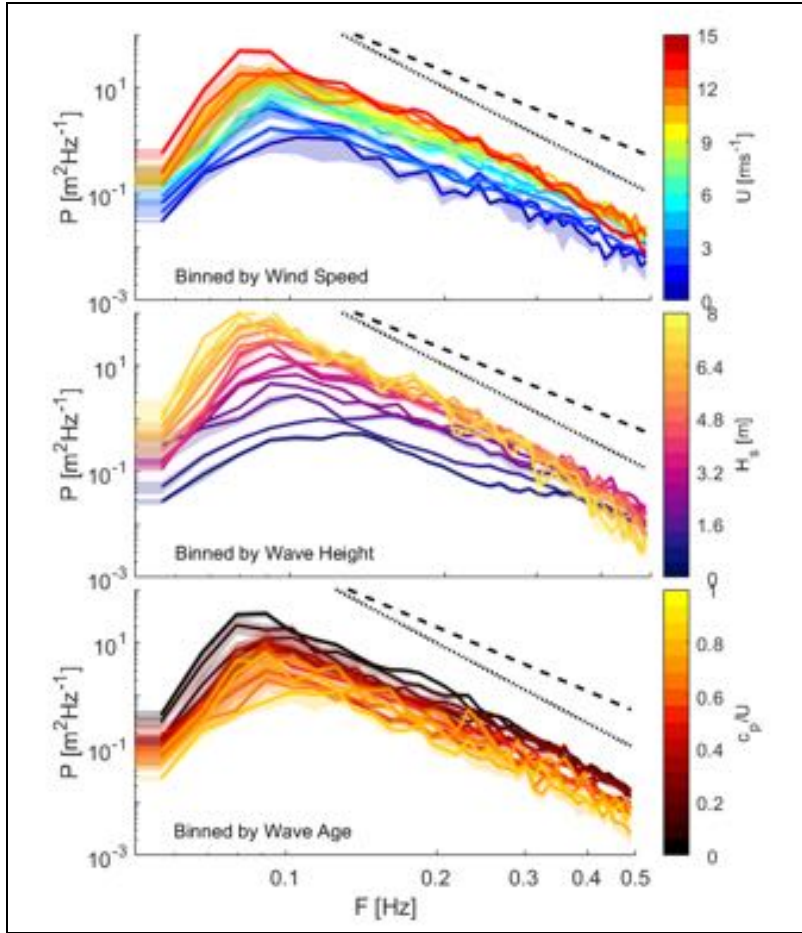


Figure 30. Surface wave spectra from SWIFT 24, binned and averaged by wind speed, significant wave height and wave age. Dashed line in each shows the spectral slope corresponding to the wind-wave equilibrium range, f^{-4} , while the dotted line gives the predicted slope for balance between wind input and wave breaking, f^{-5} . Wave spectra are well sorted by all three metrics, and spectra binned by wind speed and wave height show spectral steepening under strong forcing conditions.

Unsurprisingly, wave spectra were well sorted by wind speed and significant wave height. Figure 30 shows spectra binned and averaged as a function of wind speed, significant wave height and wave age. The slope of the high-frequency tails of the wave spectra also exhibited a dependence on wind speed and wave height. We note the latter relation is somewhat circular as significant wave height is an integral of the full wave spectra. Under steady forcing conditions, we expect a balance between wind input, nonlinear interactions and breaking wave dissipation denoted as ‘wind-wave equilibrium’. In this regime wave spectra exhibit a slope proportional to f^4 at high frequencies (Thomson et. al. 2013). Under rapid changes in forcing conditions, wind input may be balanced directly by wave breaking and studies have shown wave spectra steepen to $P \propto f^5$ in this regime (Davis et. al. 2023). Variation in spectral slope is apparent in spectra binned by wind speed. Wave spectra exhibit slopes close to f^4 at wind speeds below 5 m/s, and f^5 for wind speeds above 10 m/s. The steepening effect is emphasized further by spectra binned as a function of wave height. Increased energy in the swell band is accompanied by a decrease in

energy in the wind-sea tail of the spectra, leading to a steeper spectra. Interestingly, spectra averaged as a function of wave age do not as clearly exhibit spectral steepening. Wave age, the ratio of wave phase speed to wind speed, is typically considered to be a metric for the maturity of the wave field. We expect 'older' seas, when the wind has been blowing steadily for a long period of time, to be in equilibrium while younger seas may not be. Spectra binned as a function of wave age appear to conform to the equilibrium range spectral slope across all observed ages. However, different choices in the definition of wave age may reveal different dependencies. For example, here we have used the peak wave frequency to determine wave phase speed, but we might also consider a centroid frequency. It is also possible post-processing to reduce noise in the spectra may help discern this nuance if it is present in the data.

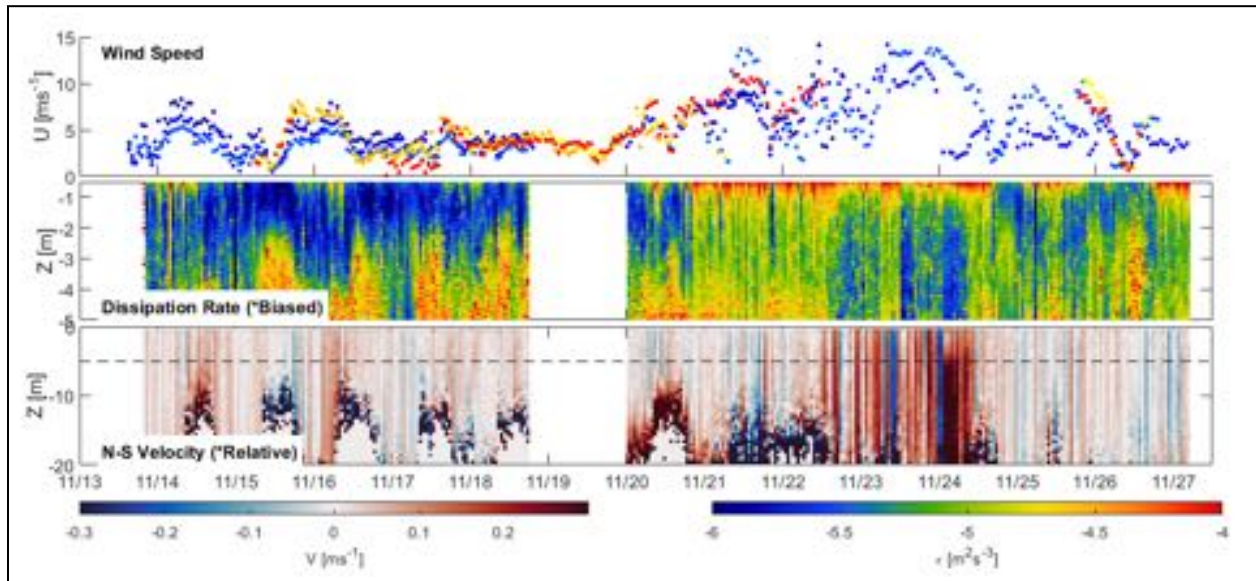


Figure 31. Near-surface turbulence from 0-5 m (biased high by waves, see text below) and relative meridional velocity from 0-20 m from SWIFT 23. Dissipation rates increase near the surface during wind events. A strong diurnal signal at depth in both dissipation rate and velocity is likely due to internal tides generated across the Jan Mayen Ridge. The high dissipation rates associated with this signal are likely due to poor data quality as a result of strong relative velocities, rather than elevated mixing.

Finally, a primary function of the SWIFT drifters is to measure profiles of near-surface turbulent kinetic energy dissipation rate, $\epsilon(z)$, in a surface-following reference frame. An example of the turbulence and velocity data measured by a single V4 SWIFT is given in Figure 31. It is important to note that telemetered $\epsilon(z)$ estimates are biased high due to wave orbital velocity contamination, which needs to be removed in post processing. The bias is depth dependent, with greater bias near the surface and decays exponentially with depth. However, some physical patterns are discernable in the telemetered data. First, $\epsilon(z)$ in the upper 2 meters increases by two orders of magnitude in response to storm forcing. Higher dissipation rates are also apparent during the weaker wind events which occurred earlier in the observation period. Because dissipation rates are biased high by wave orbital velocities, there is some confounding effect during the storm in this preliminary data, but during the calm period when waves were mild the elevated dissipation rates are presumably entirely due to the wind. At depth, a clear

diurnal signal is evident in the broadband velocity data. Other observations during the field experiment show strong internal tides generated across the Jan Mayen Ridge, suggesting this signal is likely due to internal tides as well. The high-dissipation rate estimates at depth which appear to coincide with the internal tide are likely due to poor data quality, either due to strong velocities associated with the wave or low scattering water. Post-processing will help discern whether these dissipation patterns at depth are real.

Little whorls have lesser whorls: finescale and microscale phenomenology

While it appears that mesoscale eddies are stirring both surface gradients and sub-surface spice variability along isopycnals on scales of km to tens of km, there is an equally rich story playing out at horizontal scales of meters to hundreds of meters, particularly before the storm. Both the bow chain and V-Wing data show a surprising and confusing number of phenomenological animals in the zoo at these scales. The data obtained from the bow-chain and V-wing highlighted the temperature variability in the upper 80m of the region (Figures 32,33,34). Many of the small-scale features observed here would be particularly good targets for detailed comparison with LES process modeling.

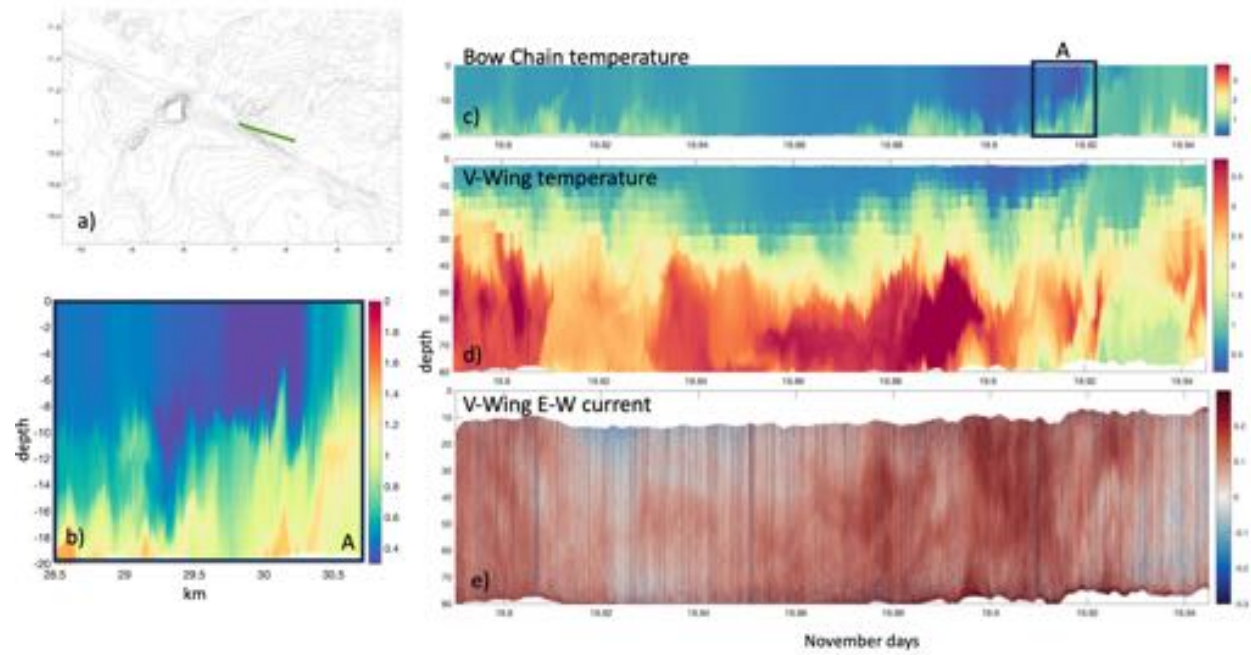


Fig 32. Example of (c) bow chain and (d) V-wing temperature data collected simultaneously before the storm (Deployment 2 in table 2), and (e) E-W velocities from the v-wing along section detailed in (a). A T-chain portion in display in b to highlight the lateral length scale of the features captured by the bow chain and the V-wing.

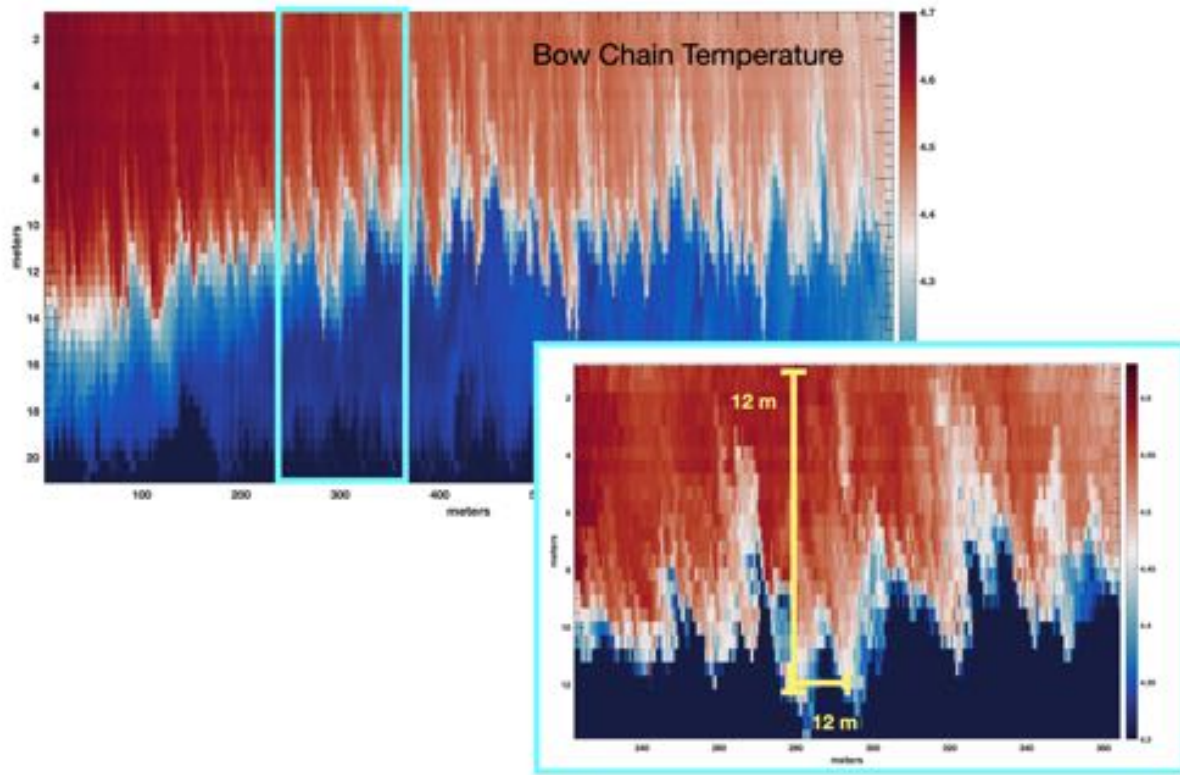


Figure 33: A section of bow-chain temperature data (plotted with along-track distance in meters) reveals what could be convective billows during a time of strong surface heat loss. A zoom in (lower panel), shows features with an order on aspect ratio.

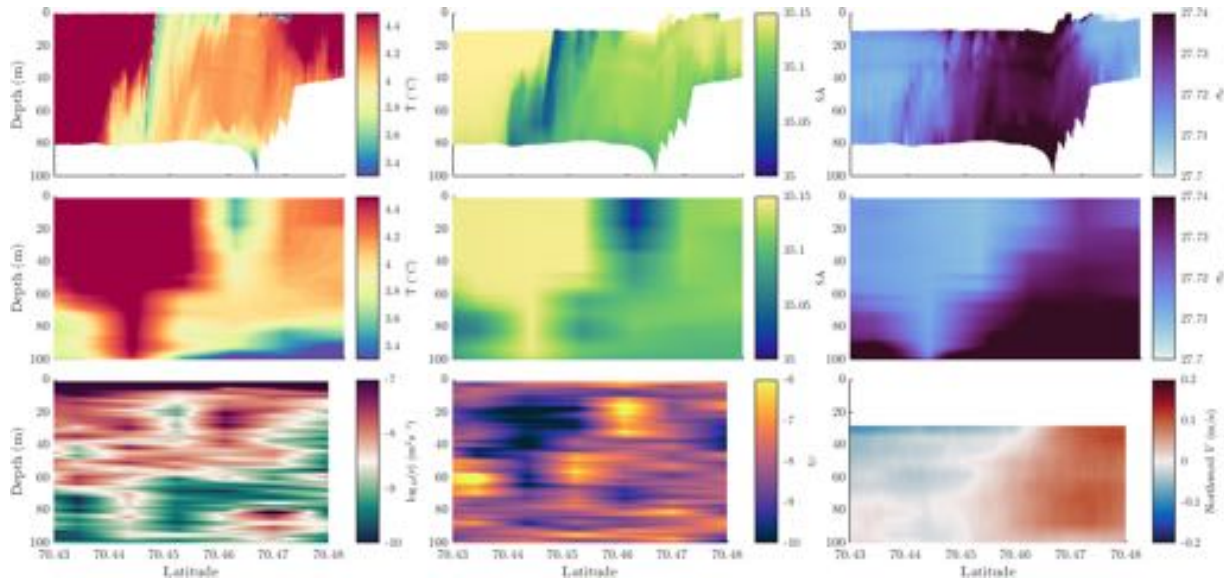


Fig 34. Post-storm frontal crossing with the V-Wing (top row) for temperature, salinity and density, compared to repeat crossing with the epsi (middle row). Including TKE dissipation (bottom row, left panel), chi (bottom row, middle panel) and shipboard velocity (bottom row right panel), which show elevated frontal dissipation and convergent velocities.

The end of the cascade: turbulent mixing

At the smallest scales, turbulent mixing dissipates kinetic energy and thermal variance, and smooths out spice anomalies. During the first part of the experiment we observed complex structure of turbulent mixing sub-surface (Fig. 35). Turbulence is elevated in a thin surface boundary layer, and in sloping layers sub-surface. Interestingly, turbulence within the sub-surface intrathermocline warm eddies is very quiet. The thermal dissipation rate is also elevated in a halo surrounding the subsurface warm layers.

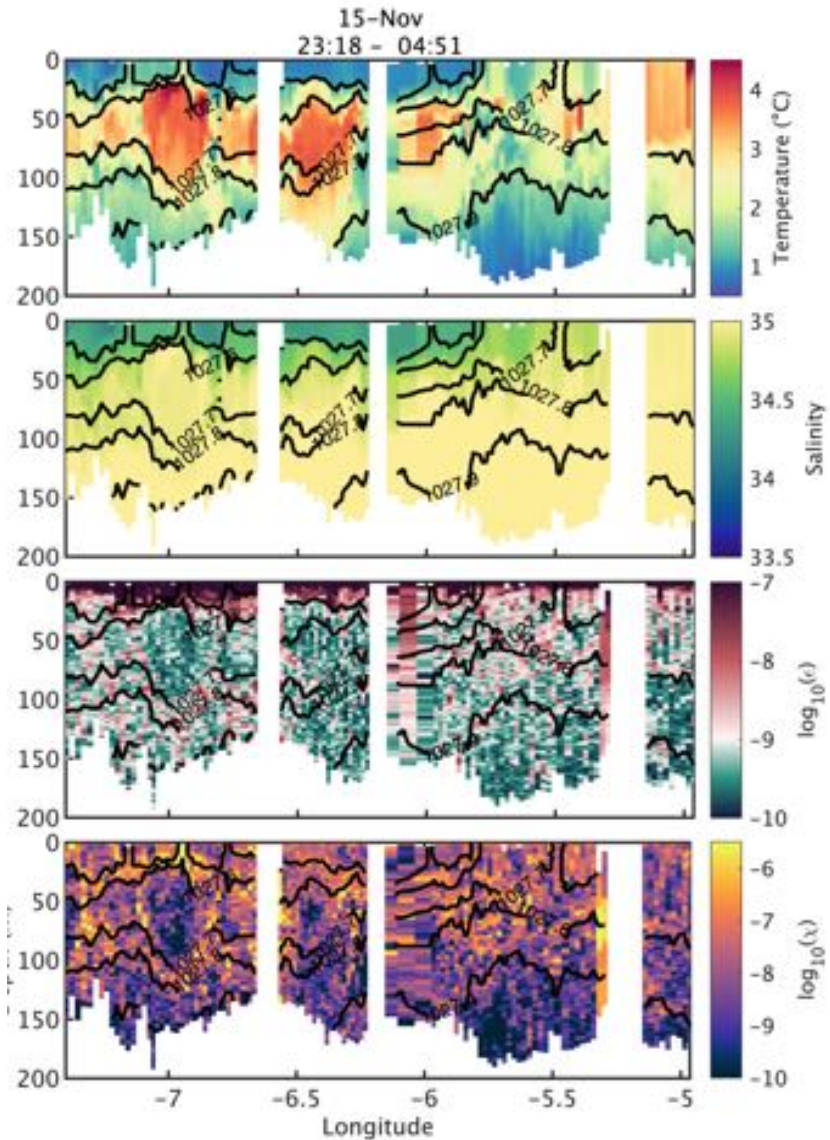


Fig 35. Temperature, absolute salinity, TKE dissipation rate, and thermal variance dissipation rate sampled along the "long section" before the storm.

Larger scale context: circumnavigation of Jan Mayen

By circumnavigating Jan Mayen, the SeaExplorer glider SEA064 saw that the bathymetric break along the Jan Mayen channel separated the warm and salty Atlantic water to the southwest from the cold and fresh Arctic water to the northeast (Figure 36). The separation of the water masses extended down to about 90 meters below which no noticeable difference in water mass property was observed. The delineation of the different surface water masses across the Jan Mayen channel is both expected and surprising as the bathymetry is at least 300m deep while the impact on water mass distribution appears to be mainly near the surface.

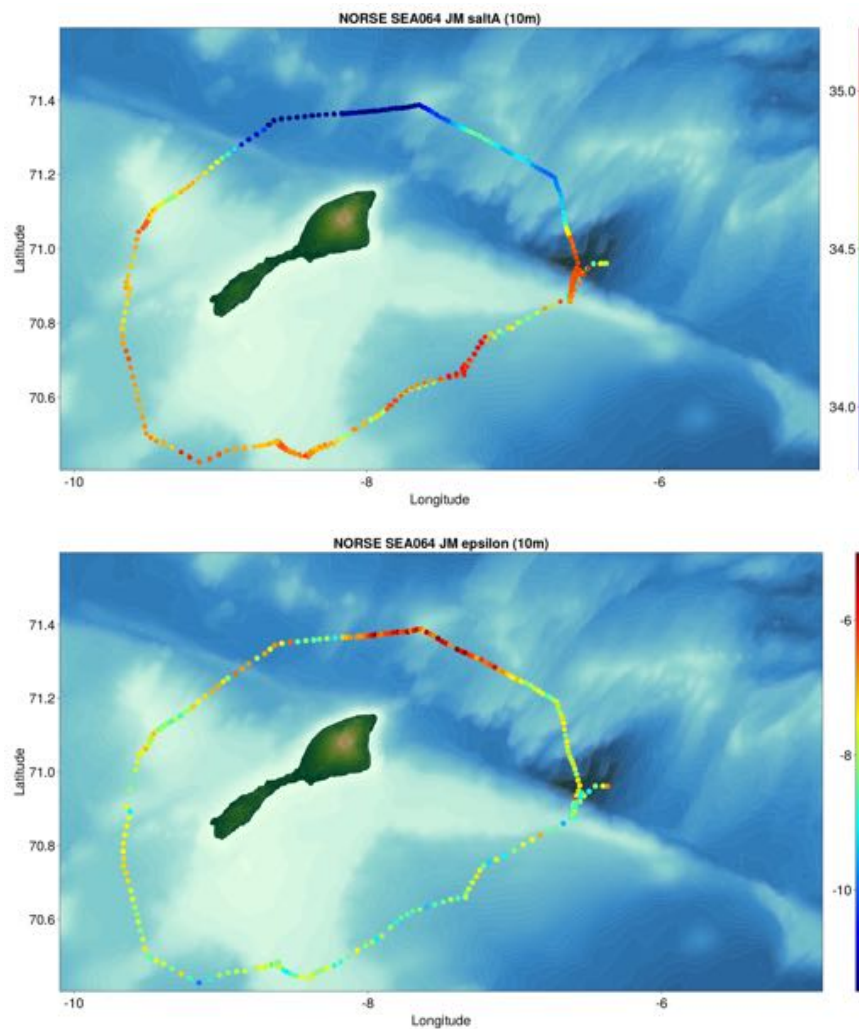


Figure 36: Glider SEA064 “French Lady” measurement of (a) absolute salinity and (b) TKE dissipation at 10 m.

As the winds picked up with the approaching storm, turbulence in the surface boundary layer began to grow, as the mixed-layer deepened. The turbulence measurements on the Sea Explorer glider give the best view of upper ocean turbulence during the storm (Fig. 37). Strong turbulence extends past 50

meters down, associated with growing shear at the base of the surface boundary layer. The storm passed when the glider was traversing through the cold and fresh Arctic water which resulted in a modest deepening of the surface mixed layer.

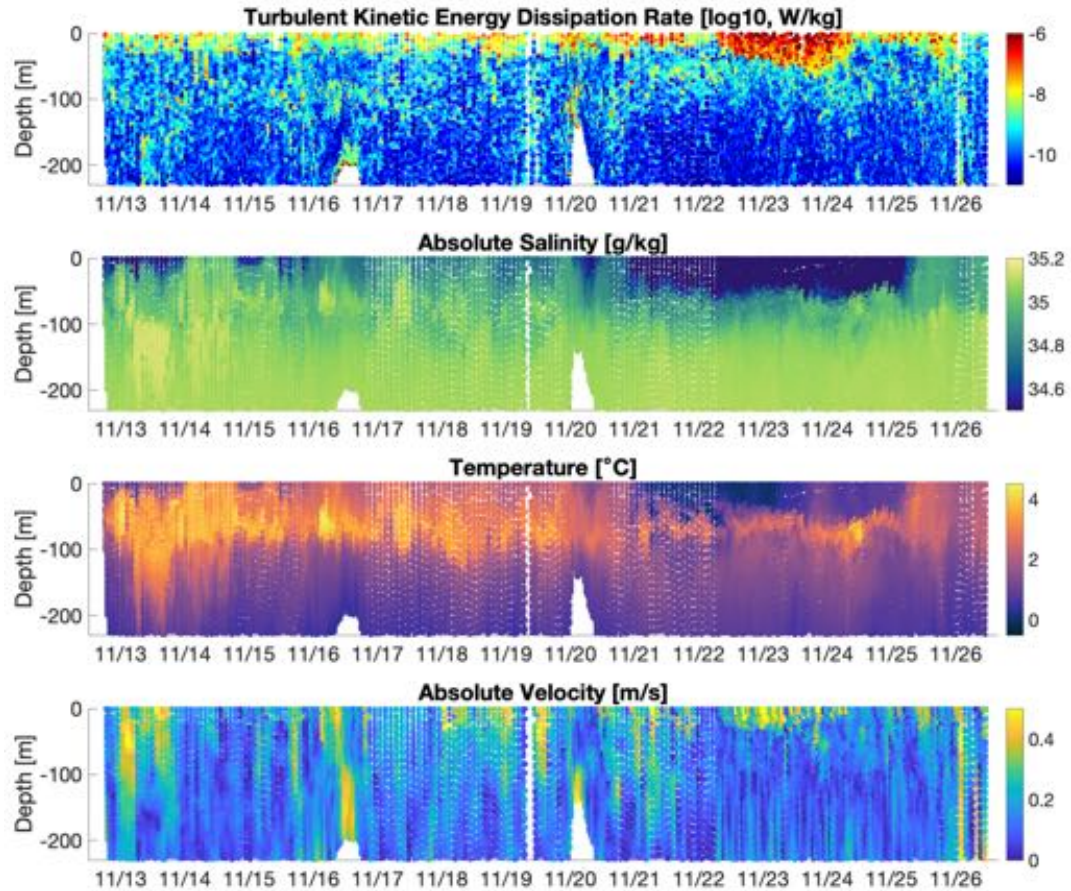


Figure 37: Telemetered observations from the SeaExplorer, showing upper 200 meters. Cold/fresh Arctic water is visible from 21-25 November, with energetic forcing from 22-24 November

[Looking deeper: Shipboard CTD and Lowered ADCP measurements](#)

At the same time that there is an intricate dance of subduction, stirring and mixing of spice in the upper ocean, a different story plays out below. A mid-depth intensified current transporting dense Arctic Intermediate Water towards the Norwegian Sea is located on the slope between the moorings. The current is associated with dense water sloping up onto the ridge.

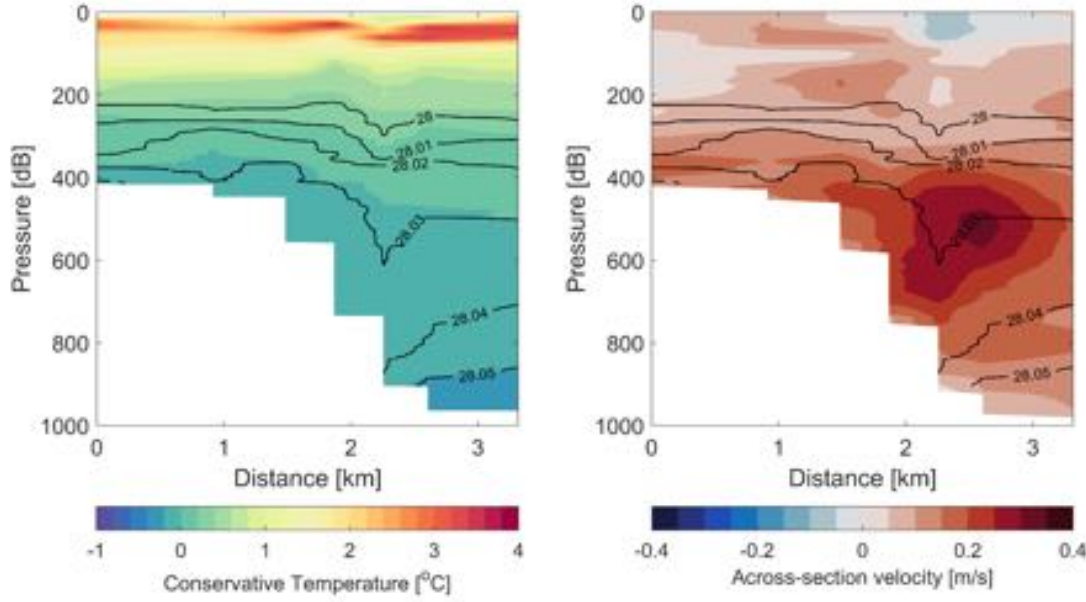


Figure 38: conservative temperature (left) and across-section velocity (right) from the shipboard CTD section in the southern side of the Jan Mayen Channel between the SW environmental mooring/PECOS and the UiB environmental mooring. Positive velocity is southeast. The black contours indicate potential density anomaly referred to the sea surface.

Lofoten Basin Eddy

Though not the primary focus this year, we did deploy a targeted set of autonomous assets in the Lofoten Basin Eddy early in the cruise. The first round of NORSE drifters were deployed in the Lofoten Basin Eddy (LBE) during the pilot in 2021 and revealed spatial patterns of kinetic energy and wind work on sub eddy scales. With these findings in mind, the 2022 deployment consisted of three times as many drifters deployed in clusters to allow for additional statistics to be computed. Furthermore, four profiling ALAMO (Air-Launched Autonomous Micro Observer) floats were deployed to tie in the subsurface. Based on the results from the 2021 and 2022 deployments, the plan for 2023 was to deploy an array (sized in between the previous two) of surface drifters and four subsurface ALTO floats with microstructure sensors.

The 2023 array was deployed as three clusters, one in the center and one on either side of the center cluster approximately 10km radial distance away to ensure maximum entrainment. The drifter clusters each had an ALTO float in the center surrounded by four SVPs in a 500m radius circle around it (the drifters were deployed north/south/east/west of the center). The center cluster had one additional ALTO float as well as one MiniMet and one DWSD, and the northernmost cluster also had one MiniMet and one DWSD.

The 16 piece (12 SVPs, 2 MiniMets and 2 DWSD) surface drifter array deployed in the LBE stayed intact for two full weeks. On November 22nd a low pressure moved in over the Jan Mayen and Lofoten Basin area, and R/V Kronprins Haakon paused science operations and sought shelter behind Jan Mayen.

The drifters in the LBE were dispersed by the storm. About half of the drifters stayed in the eddy while the other half exited the eddy and moved northeast/southeast. Bottom right panel in the figure below show the drifters in the LBE and the non recovered drifters deployed around Jan Mayen.

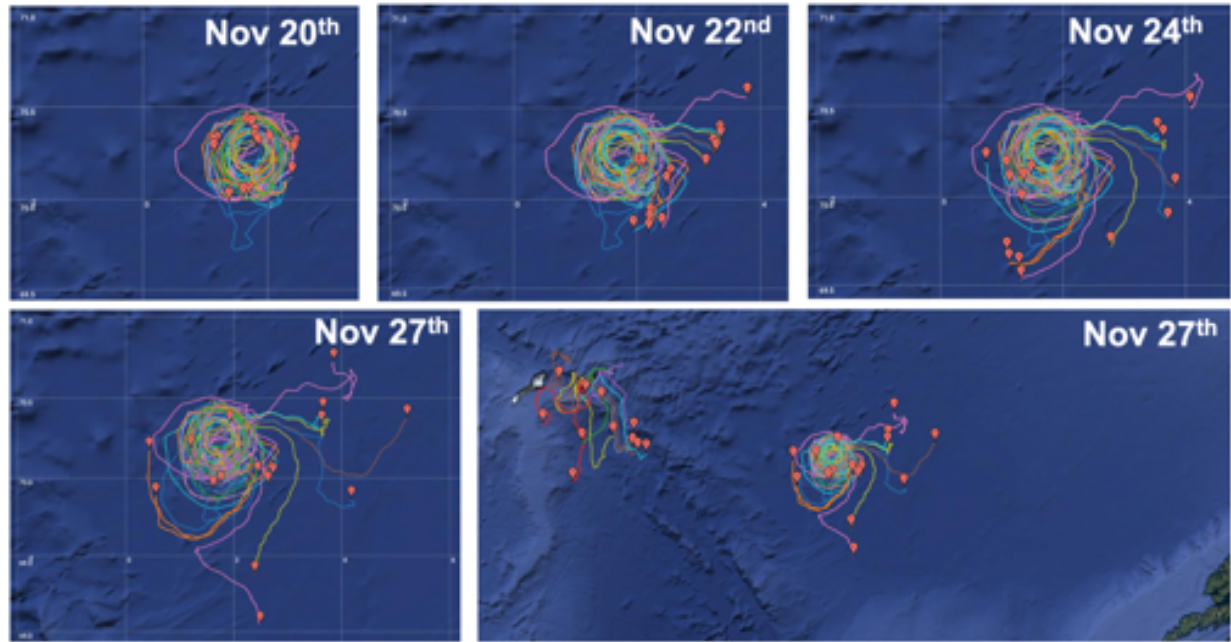


Figure 39: NORSE 2023 surface drifter locations November 20th - 27th.

Three out of four ALTO floats were still in the Lofoten Basin Eddy sampling when the R/V Kronprins Haakon approached the dock in Tromsø. The microstructure data is being processed by the team at WHOI. A figure of one of the floats' temperature over its approximately 200 dives since deployment show plenty of interesting structure.

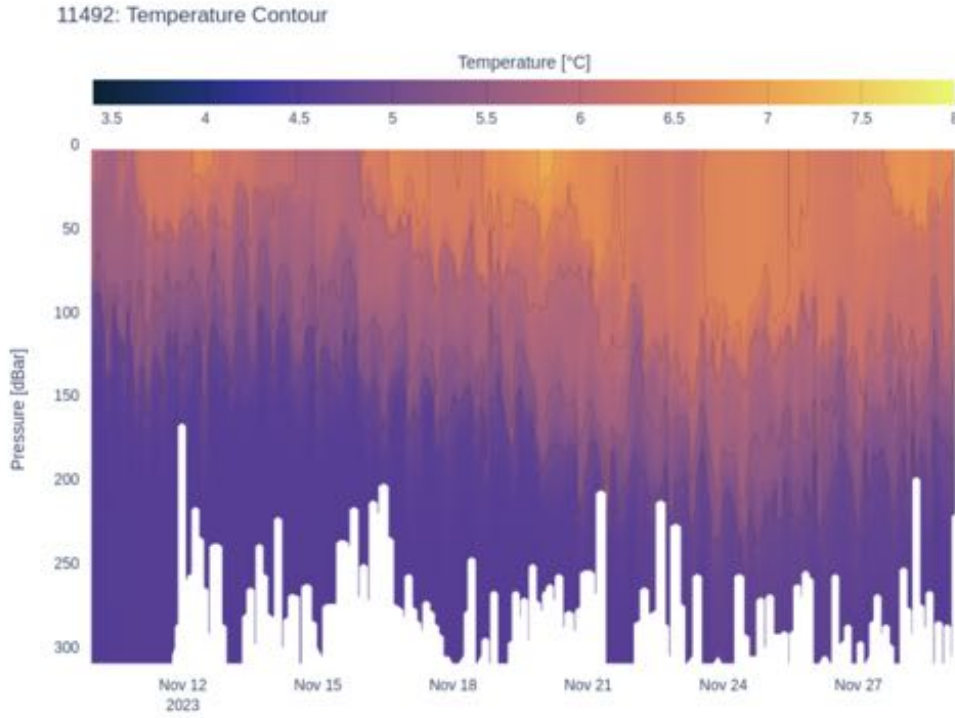


Figure 40: Alto Float 11492 temperature from the last two weeks of November 2023, within the Lofoten Basin Eddy

Year-long records: Acoustics

The PECOS array collected 390 days of data in scheduled recording mode, which recorded for 24 minutes every four hours. Two additional collections were made in continuous recording mode, including a three-hour recording during the 2022 IOP and a 12-hour recording during the 2023 IOP. PECOS had a sampling rate of 8192 Hz, and the vertical array hydrophones spanned the water column from 49 to 419 m. The PECOS data will be used to study acoustic propagation and ambient sound in the region near Jan Mayen.

The PECOS array recorded the 109 signals transmitted from the moored source, which was located 42 km away on the north side of Jan Mayen Channel. The moored source broadcast a 135-second long chirp in the 500 to 1500 Hz frequency band. A subset of the pulsed compressed receptions are shown in the figure below. The top left panel highlights the ray-like convergence zone paths (lines) and the mode-like ducted sound path (circle). The ducted path fades, disappears, reappears, and strengthens over the 18 days of receptions shown in the figure. The changes in the arrival pattern are due to variations in the water column properties over the course of the experiment. We will seek to fully characterize the acoustic arrivals using forward modeling supported by oceanographic measurements from the moorings and the 2022 IOP.

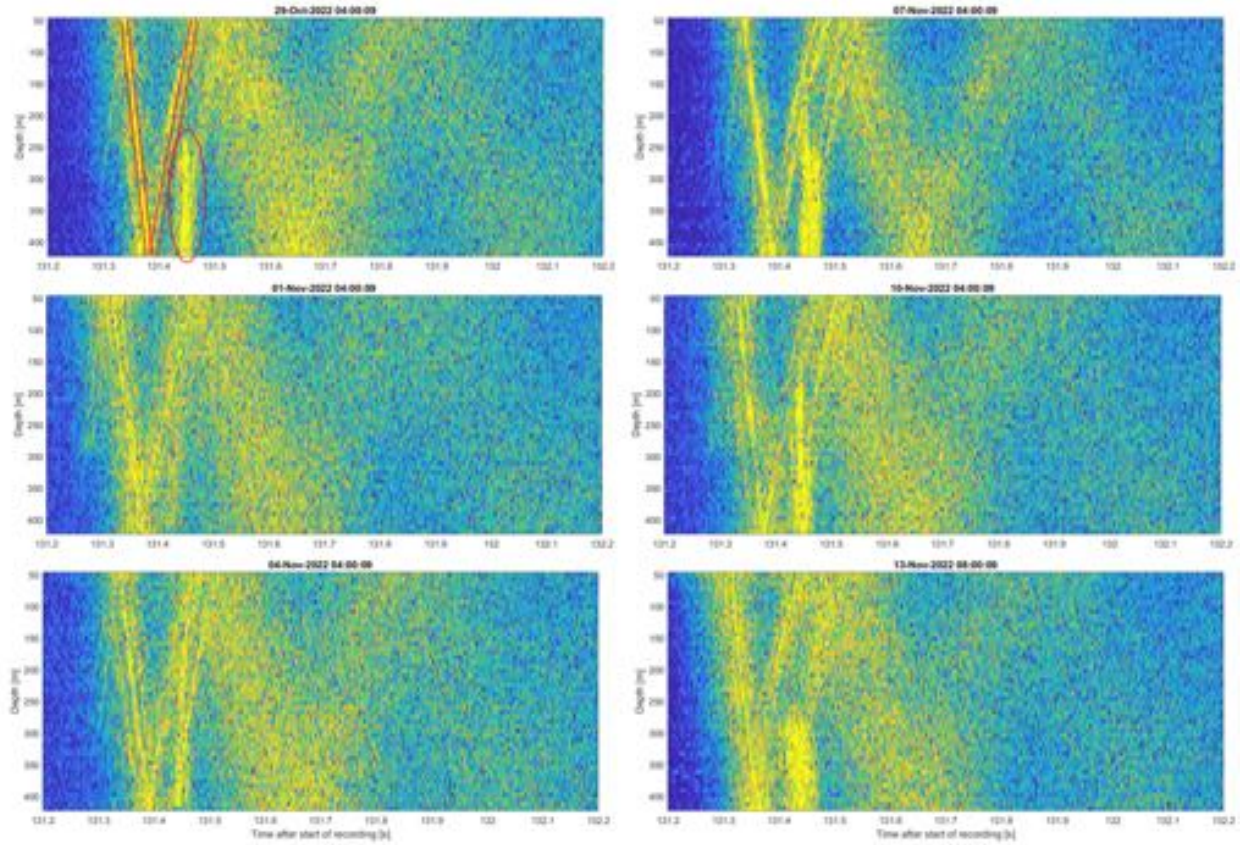


Figure 41: A subset of the 109 receptions of pulse compressed signals from the moored source on the PECOS array. These receptions were recorded three days apart. The top left panel highlights the ray-like convergence zone paths (lines) and the mode-like ducted sound path (circle). The ducted path fades and disappears due to variations in the water column properties over the course of the experiment.

The PECOS array also recorded the transmission sequence broadcast by the DBASIS source in 2022 and 2023. The DBASIS source broadcasted a series of 4.1-second-long chirps in the 610 to 890 Hz frequency band. A subset of the signals collected in November 2023 are in Figure 42. PECOS recorded the DBASIS source for approximately five days before the moorings were recovered. During this time, PECOS was switched into continuous recording mode and collected 12 consecutive hours of DBASIS signals. Variations in the receptions are caused by the changes in the water column properties as well as the position of the drifting source. We will seek to fully characterize the acoustic arrivals using forward modeling supported by oceanographic measurements from the moorings and the 2023 IOP. Furthermore, we will also investigate the 2022 DBASIS signals recorded on PECOS. The propagation environment as described by the water column properties was significantly different between the two different years: in the fall of 2022, the water column included a warm surface layer such that the water column sound speed profile contained one subsurface duct centered around 200 m; in the fall of 2023, there was surface temperature maximum that formed a surface duct in the upper 10 to 20 m as well as the subsurface duct typical for the season in this region.

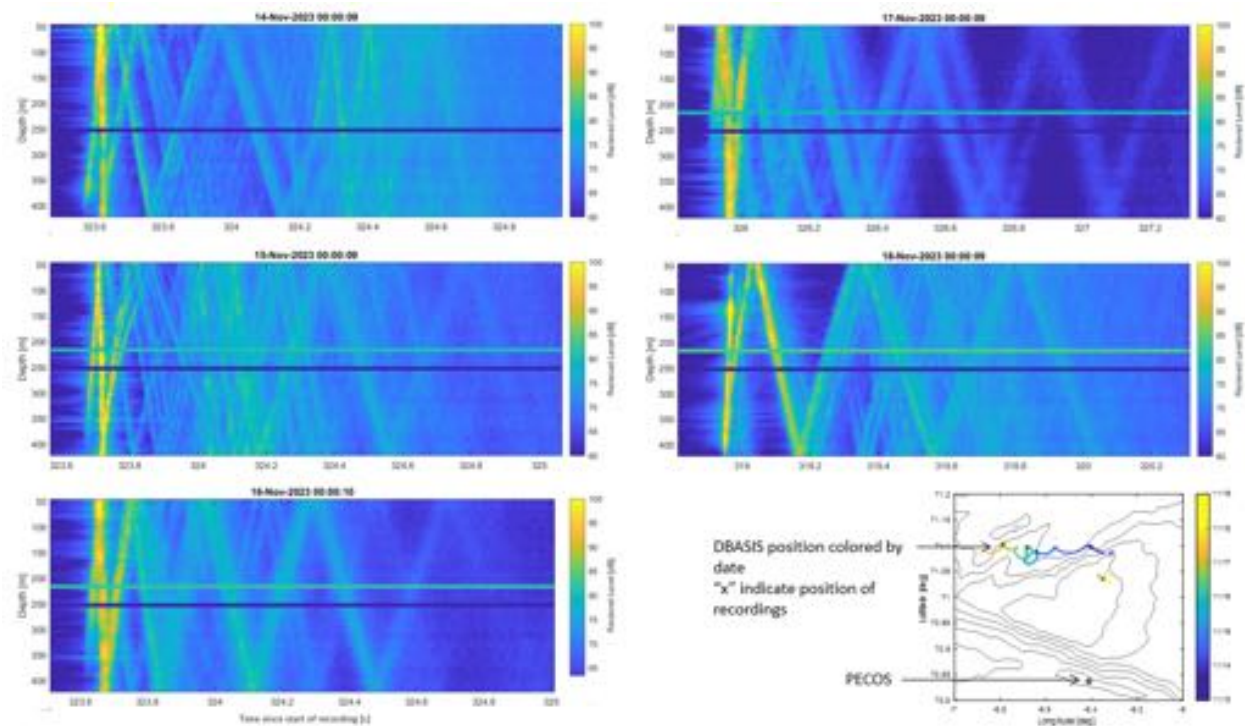


Figure 42: Subset of signals broadcast by the DBASIS source recorded by PECOS in November 2023. Approximately 35 pulse-compressed signals were averaged together to increase SNR. Variations in the receptions are caused by the changes in the water column properties as well as the position of the drifting source. The two bad channels are evident in the PECOS data.

An initial survey of the PECOS ambient sound data from its 390-day deployment is shown in Figure 43. The upper panel shows the 25th percentile level calculated from 375 seconds of data once a day. Using these data, some of the dominant ambient sound generation mechanisms were identified. Above 1 kHz, the ambient sound level is well correlated with wind speed as observed from the wind speed data from the NCEP/NCAR 40-year reanalysis project overlaid on the acoustic data. Sustained higher wind speeds between December and March are associated with the higher levels of sound observed in the winter season.

Below a few hundred hertz, several sources of ambient sound were identified. The elevated level in the 20 Hz band is attributed to fin whale (*Balaenoptera physalus*) vocalizations. Fin whales are more common at high latitudes during summer and at low latitudes during winter, although some fin whales remain at high latitudes during winter or at low latitudes during summer. Their vocalizations are seasonally present in the PECOS data, increasing in intensity through the fall, showing sustained presence through the winter, and disappearing in the spring. Beginning in mid-April and continuing through mid-September, seismic profiling (airguns) are observed in the data. This interactive map (https://factmaps.npd.no/factmaps/3_0/) shows a number of active 3D seismic survey sites in the Norwegian Sea that are a likely source of the observed signals. Distant shipping, a ubiquitous source of low-frequency sound is also indicated in the figure. The lower panels of the figure show two 60-second

spectrograms from 25 November 2022 when the fin whale vocalizations are present, and from 7 May 2023 when the seismic profiling is the primary source of low frequency sound.

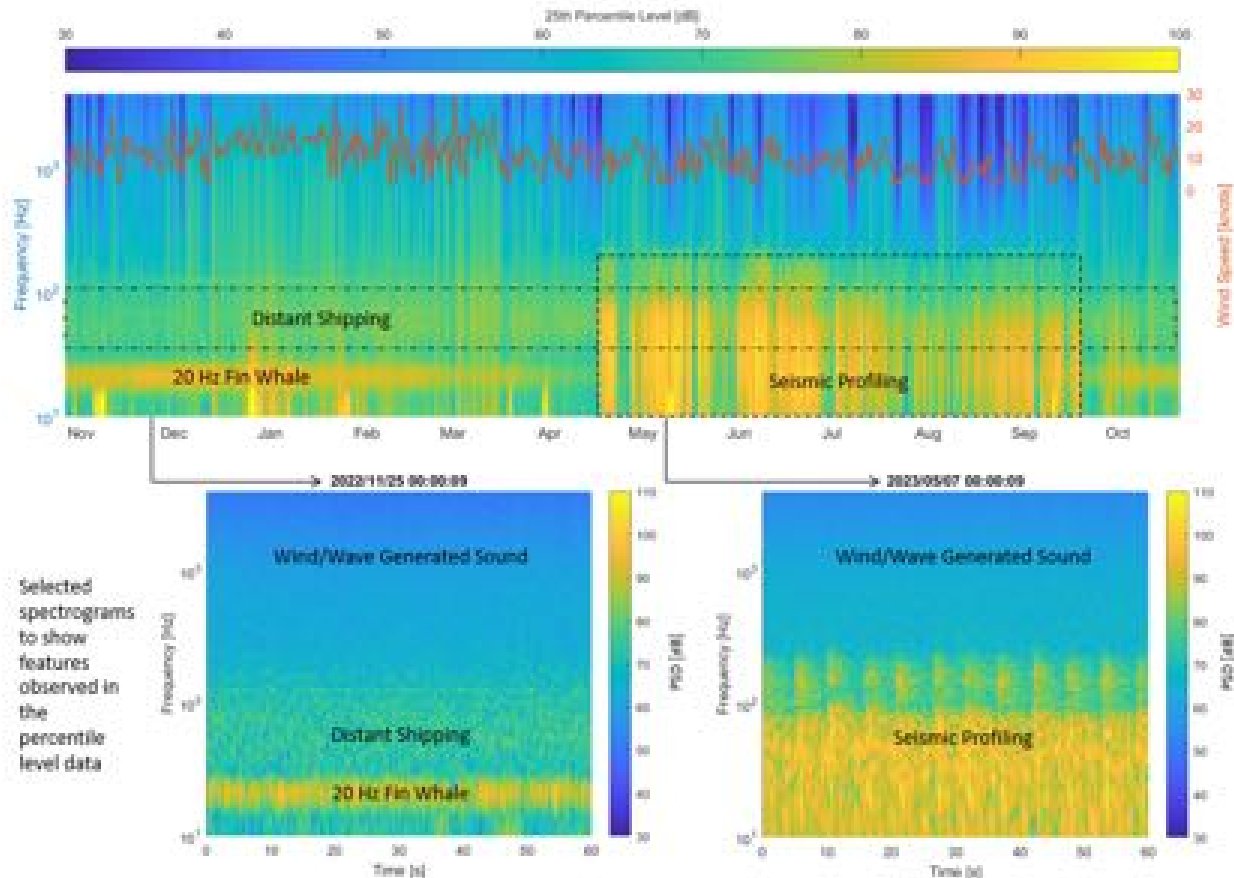


Figure 43: Ambient sound measured by PECOS at a depth of 78 m. The top panel shows the 25th percentile level calculated from 375 seconds of data from one recording each day. Above 1 kHz, the ambient sound level is well correlated with wind speed. The dominant sound generation mechanisms for other frequency ranges and times are labeled on the figure. The bottom shows spectrograms from two different time periods.

Year-long record: Physical Oceanography

The shallow water environmental (SWE) mooring captured the transport of heat and freshwater over Jan Mayen ridge. The winter months (NDJ) are associated with a northward transport of warm water over the ridge that is consistent across the entire water column. This northward transport of heat is seen in the surface waters of the UIB mooring, but not in the source mooring. Spring (FMA) currents are generally smaller and change direction from northward to southward. In May, surface waters see warmer temperatures with a southwestward transport, while deeper waters continue to see a cold northward transport over the ridge.

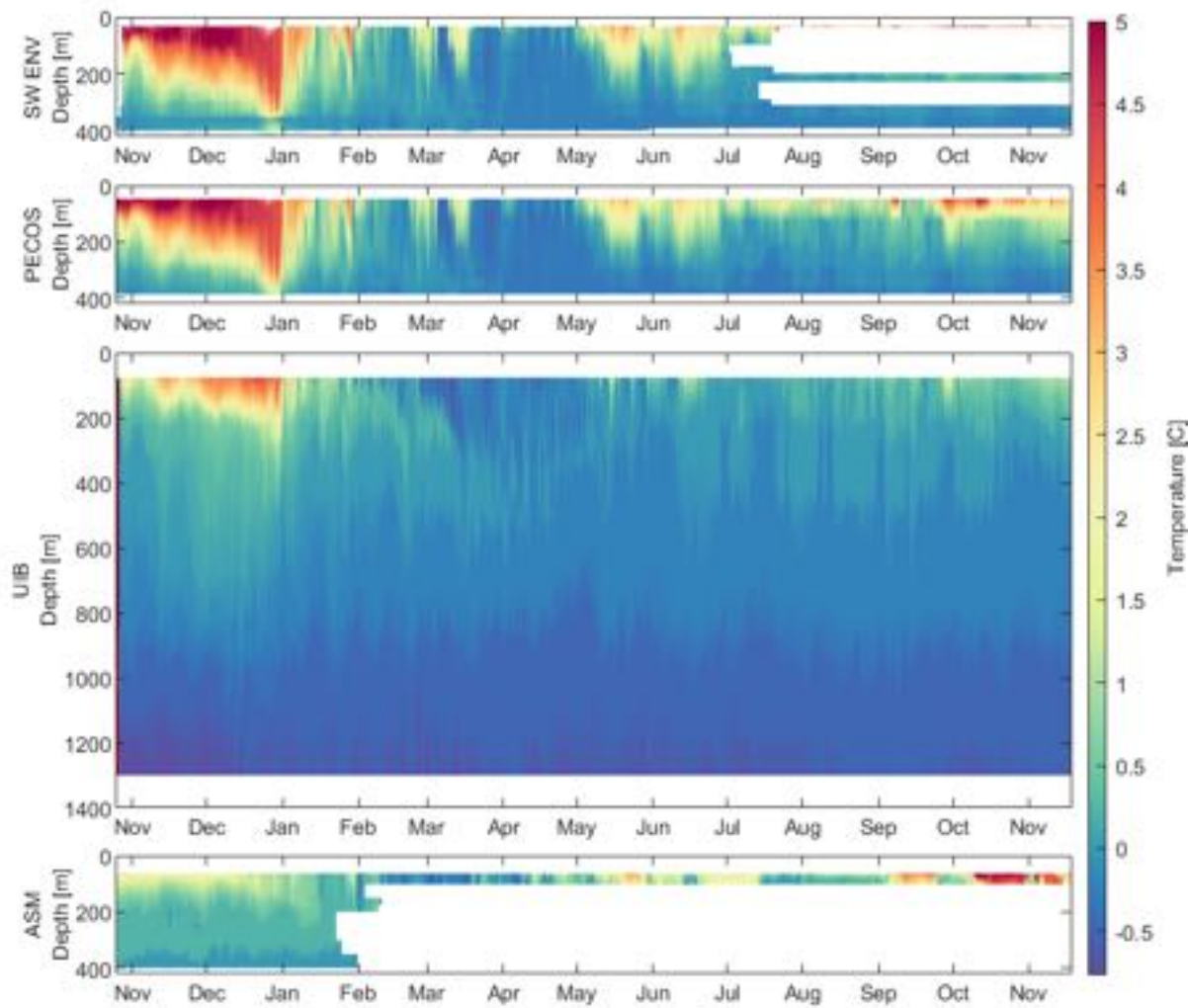


Figure 44: Temperature data recorded by the four moorings deployed in support of NORSE. The SWE, PECOS, and UIB moorings were located on the south side of Jan Mayen Channel, and the ASM mooring was located on the north side of the channel.

| Mooring | Type | Lat [deg N] | Lon [deg W] | Depth [m] | Uncert [m] |
|------------------------|---------------|-------------|-------------|-----------|------------|
| PECOS | Triangulation | 70.836847 | -6.411678 | 413 | 3 |
| PECOS Recovery Mooring | Anchor drop | 70.841858 | -6.401289 | 485 | n/a |
| Acoustic Source | Triangulation | 71.211565 | -6.298711 | 1165 | 10 |
| SW Environmental | Anchor drop | 70.831946 | -6.399105 | 413 | n/a |
| UIB Environmental | Anchor drop | 70.869161 | -6.415010 | 1505 | n/a |

Table with mooring locations.

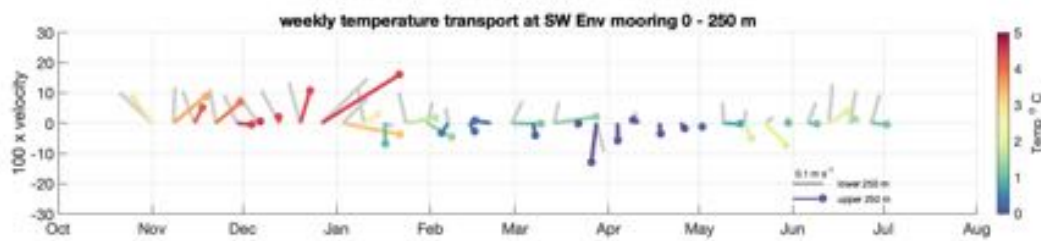
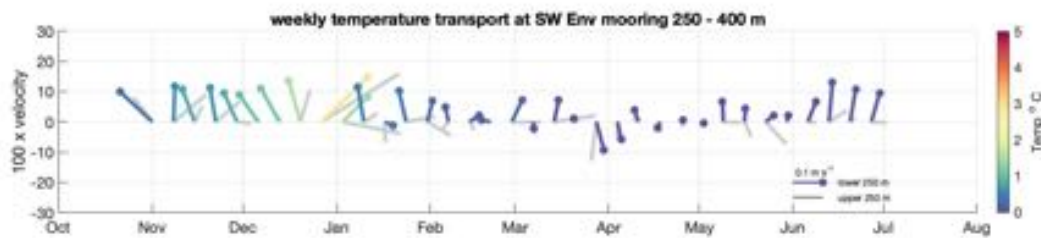


Figure 45. Heat transport over Jan Mayen Ridge – weekly temperature and velocity measured by the SWE mooring. top: lower water column (250-380 m). bottom: upper (30-250 m). Vectors are low passed weekly current velocities and are colored by temperature.

Internal tides near Jan Mayen Ridge

Though not a goal of the sampling plan, we could not help to notice the extremely strong internal tides near the steep Jan Mayen topography. At this latitude, the semidiurnal internal tide can still propagate, but with a very slugging group velocity. This allows the potential for an interesting situation in which internal waves may be semi-trapped to the ridge, one in which instead of the balance between generation and propagation there may be a more complicated balance between generation, local dissipation, along-topography propagation and weak radiation.

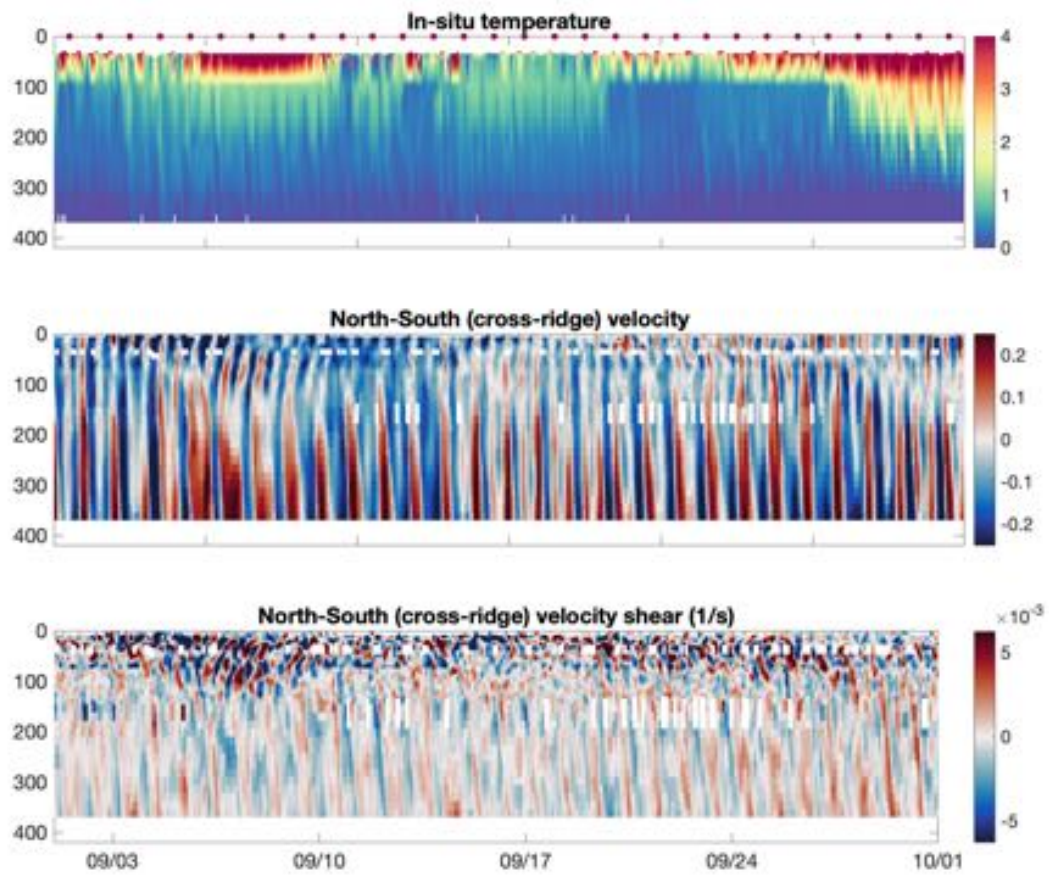


Figure 46: SWE mooring in-situ temperature (top panel), cross-ridge velocity (center panel) and cross-ridge vertical shear (bottom panel) September 2023. The temperature record is a synthetic product derived from all temperature recording instruments on the SWE mooring plus the nearby PECOS mooring. The velocity record is constructed from the upward looking Signature 500 ADCP and downward looking WHS300 ADCPs on the SWE stablemoor (nominal pressure = 31 dbar) and the downward looking cage mounted LR75 at nominal pressure of 73 dbar. Lower panels have been de-spiked using a 2D 3x3 median filter for visualization.

Larger-scale context: Glider Freya Transit from Iceland

Slocum glider SN506 (“Freya”) was equipped with a Rockland Scientific Microrider SN133 and an onboard turbulence processor that allowed for satellite transmission of turbulent kinetic energy dissipation rates (W/kg). Freya was deployed from the *R/V Bjarni Sæmundsson* on 14 August 2023 by Andreas Macrander of the Marine and Freshwater Institute of Iceland. It then executed a 90 day mission to the Jan Mayen Ridge area, first arriving at Jan Mayen Ridge approximately 15 September 2023 and for the remainder of the mission shuttled back and forth between the PECOS/SWE mooring region to the ARM mooring region. It then made 18 transits (9 round trips) between 15 September and 12 November 2023 and was recovered without incident via the workboat of the *RV Kronprins Haakon*.

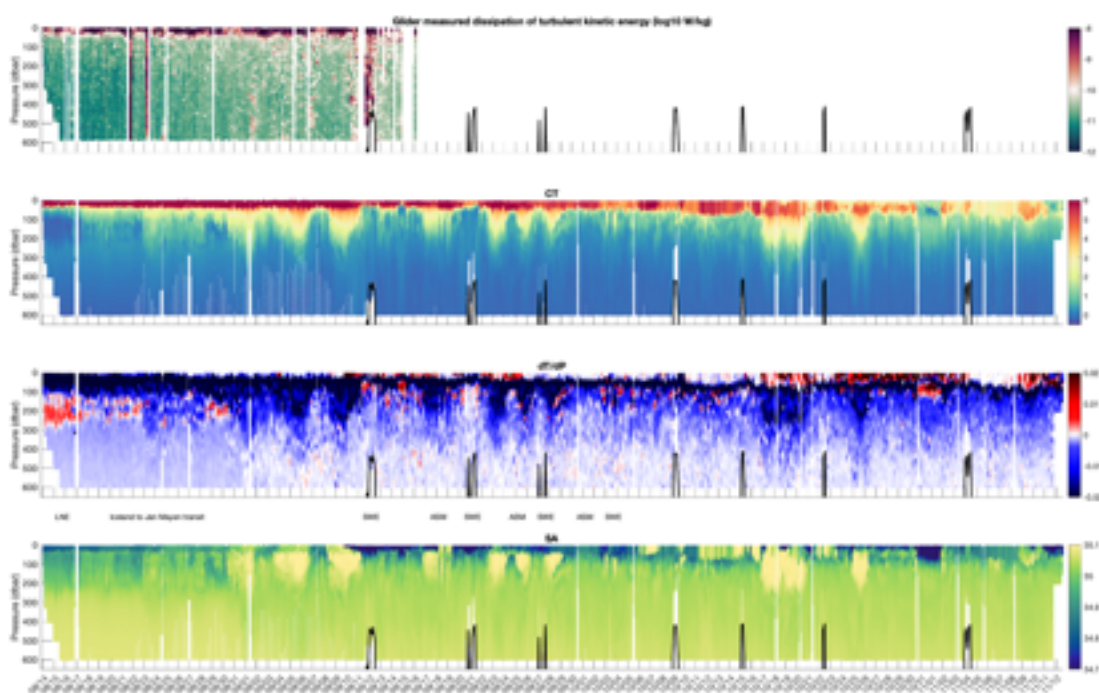


Figure 47: Measurement by slocum glider “Freya”. Top panel: Depth-time profiles of turbulent kinetic energy dissipation (W/kg). Second panel: conservative temperature (°C). Third panel: vertical gradient of in-situ temperature as recorded by the glider Seabird sensor (°C/m). Fourth panel: Absolute Salinity (g/kg).

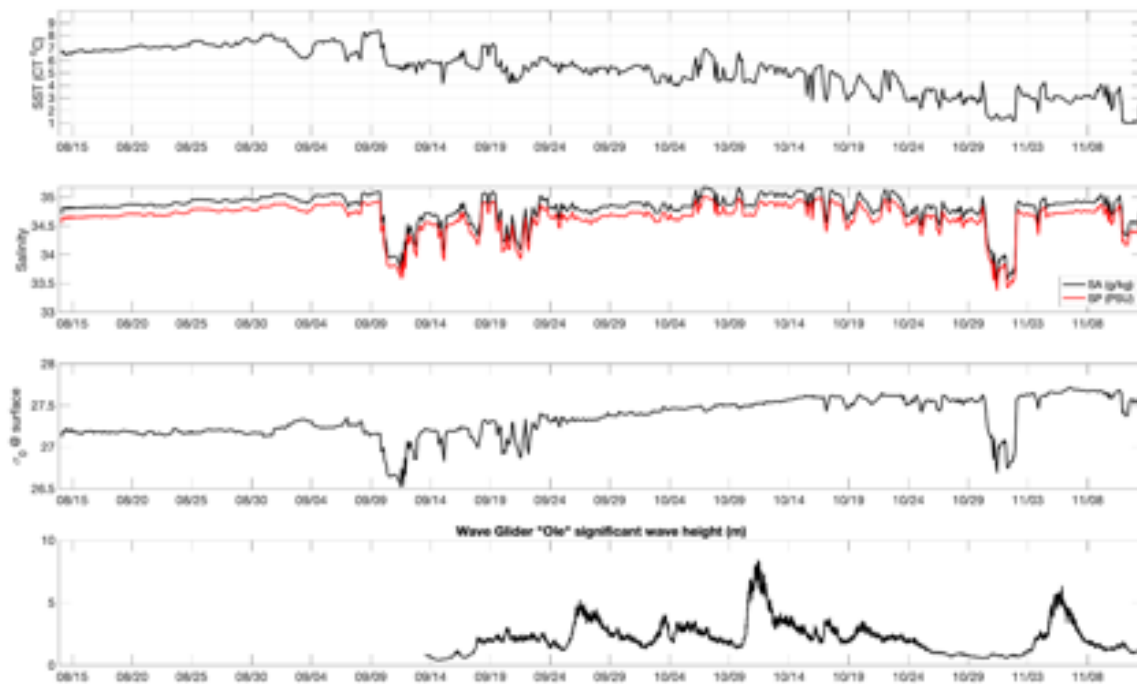


Figure 48: Summary of surface water properties measured by Slocum glider Freya's during its transit to Jan Mayen and subsequent shuttling between PECOS and ASM (top three panels) and significant wave height measured.

The onboard turbulence processor recorded 125 profiles of dissipation rate until 16 September when the microrider and turbulence processor shut down for unknown reasons. This event occurred shortly after its first transit of Jan Mayen ridge and revealed full depth enhancement of turbulent dissipation of 3 orders of magnitude above its noise floor of 10^{-11} W/kg over multiple profiles as it crossed the ridge during the 9-13 September time period. The CTD package on the glider continued to operate until its recovery 12 November. Throughout the transit from Iceland and during its sampling in the Jan Mayen region, the glider recorded sub-surface increases in temperature with depth. Near Iceland, the region of subsurface temperature maximum was between 100-300m whereas in the Jan Mayen region it was centered at approximately 50m. Note also that the glider recorded temperature maximum was weaker than that recorded from shipboard profiling instruments.

The glider recorded subsurface maximum temperature between the two moorings is most evident after Oct 15 and persisted intermittently until recovery Nov 12. However during that time the subsurface temperature maximum was frequently interrupted by the appearance of cooler and fresher polar waters. Additionally during the 4-9 November storm the upper ocean appears to mix down and into the subsurface temperature maximum such that it no longer appears as an extrema. By 9 November the subsurface maximum temperature had returned.

Larger-scale context: Wave Glider Ole Transit from Iceland

Waveglider SV3-253 ("Ole") was deployed from the *R/V Árni Friðriksson* by Arnþór Bragi Kristjánsson on SEP 13 approximately 160 nm west of Jan Mayen. It's sensor loadout consists of a Vaisala WXT (wind speed, wind direction, barometric pressure, temperature, and relative humidity), CORDC waves sensing package (wave height, period, and direction), and Teledyne 300kHz ADCP for current measurements up to 100m depth. The vehicle was modified to utilize higher capacity primary lithium batteries and allow operations in this solar deficient region. This switch in battery chemistries increased overall energy capacity by fourfold.

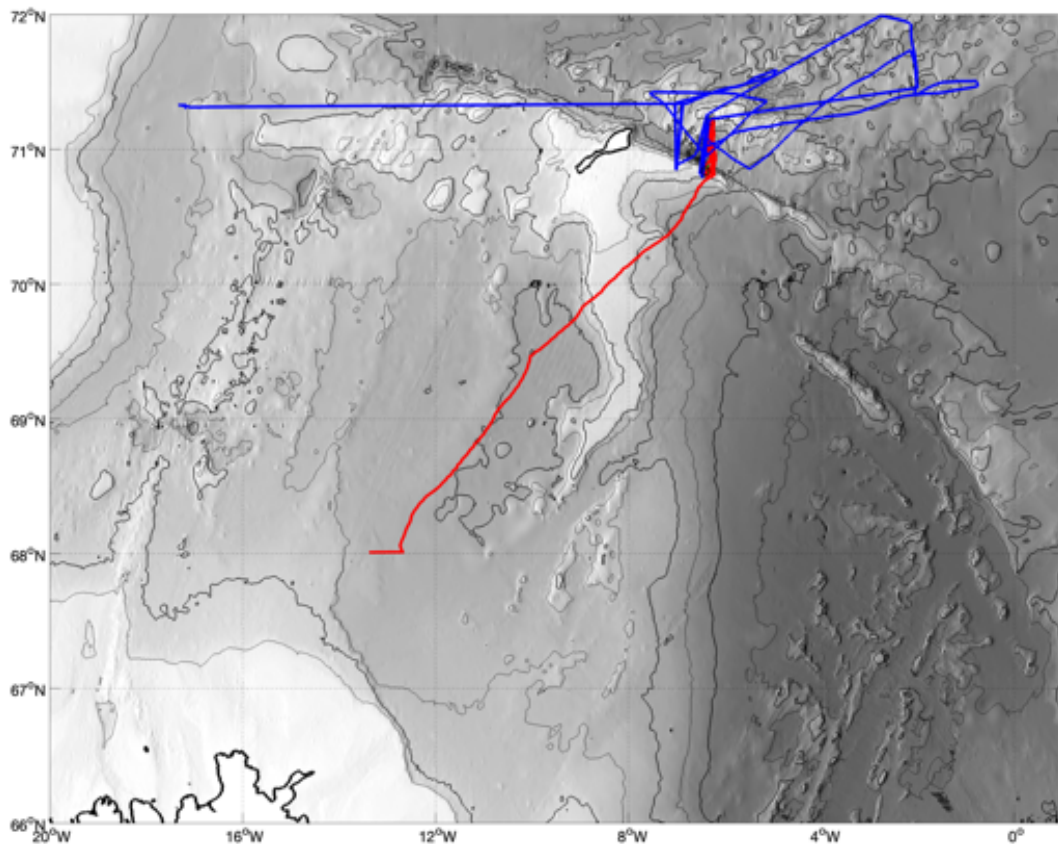


Figure 49: Tracks of Waveglider "Ole" (blue trace) and Slocum glider "Freya" (red trace) during their missions.

Ole arrived at the mooring regions on SEP 20 and started a N-S transect between them. MET and waves sensing were active starting from SEP 13. ADCP data collection was active between OCT 06 and NOV 05, continuously recording and reporting 10min averages during this time. For the periods of OCT 10 - OCT 16 and NOV 4 - NOV 7, Ole headed into the waves to prioritize survivability (sea state exceeding WMO 5). At the vehicle's 1-2kt speeds, a transect could be completed every 16 hours; about 35 crossings were completed between the moorings with the ADCP active. The waveglider was recovered on NOV 12 yielding a total uptime of 60 days.

6. Educational activities during the cruise

We had 2 (stemseas) undergraduates, 8 graduate students and 5 postdocs participating in the cruise. They were involved in every aspect of cruise planning, data gathering, and scientific discussions.

7. Science Party Personnel

| Name | Role | Institution |
|------------------------|-----------|--|
| Jennifer MacKinnon | Chief Sci | Scripps Institution of Oceanography |
| Megan Ballard | PI | University of Texas |
| Leah Johnson | PI | University of Washington |
| Pierre Poulain | PI | CMRE |
| Harper Simmons | PI | University of Washington |
| Ailin Brakstad | Scientist | University of Bergen |
| Nicole Couto | Scientist | Scripps Institution of Oceanography |
| Laur Ferris | Postdoc | Applied Physics Laboratory - UW / VIMS |
| Leo Middleton | Postdoc | WHOI |
| André Palóczy | Postdoc | University of Oslo |
| Filipe Pereira | Postdoc | Scripps Institution of Oceanography |
| Alejandra Sanchez-Rios | Postdoc | Scripps Institution of Oceanography |
| Olivia Adams | Student | Pennsylvania State University |
| Emily An | Student | University of Florida |
| Kerstin Bergentz | Student | Scripps Institution of Oceanography |
| Caique Dias Luko | Student | Scripps Institution of Oceanography |
| Erika Giorgi | Student | University of Bergen |
| Ankitha Kannad | Student | Scripps Institution of Oceanography |
| Malcolm LeClair | Student | University of Washington |
| Devon Northcott | Student | Scripps Institution of Oceanography |
| Andrea R-M-F | Student | Scripps Institution of Oceanography |
| Nicole Trenholm | Student | U. Maryland Center for Environmental Science |
| Marina Ampola Rella | Engineer | CMRE |

| | | |
|-------------------|----------|-------------------------------------|
| Marco Bernardini | Engineer | CMRE |
| Helen Dufel | Engineer | Scripps Institution of Oceanography |
| John Eischer | Engineer | University of Texas |
| Emerson Hasbrouck | Engineer | WHOI |
| Sean Lastuka | Engineer | Scripps Institution of Oceanography |
| Joe Talbert | Engineer | Applied Physics Laboratory - UW |
| Eli Willard | Engineer | University of Texas |

Table: Personnel

8. Appendix

Detailed Schedule

8-9 November: Lofoten Basin Eddy. After two smooth days of loading, we left Tromsø at 0400 on 8 November, steaming towards the Lofoten Basin Eddy. We arrived at the eddy mid-day on the 9th. We recovered the University of Bergen glider (which had been out for a while) and then spent around six hours surveying the LBE at 10 knots to pin down the eddy structure and location of the center. We had decided beforehand not to do any appreciable shipboard work here this year, but to deploy enough autonomous assets to still be able to tell an interesting story. Following the fast survey, we deployed surface drifters and 4 Alto profiling microstructure floats. The hope here is that the clusters of surface drifters will tell us about not only the smaller scales of vorticity structure within the eddy center, but also about how the input of wind energy into near-inertial motions responds to those structures. The Alto floats will then measure patterns of turbulence produced by the resultant downward propagating near-inertial internal waves. All assets deployed are telemetering data, and do not need to be recovered.

10-11 November: Brief Interruption. Just as we were about to leave to head to Jan Mayen, we learned that one of the crew members had a dying parent. We diverted to drop them in port in the Lofoten islands, then headed to Jan Mayen. In total we lost about 2 days of time, which we chalked up to 'weather' days.

12-13 Jan Mayen Initial Surveys. The first goal at Jan Mayen was to recovery a glider and deploy a couple more gliders, and then scope out the lay of the land initially with a fast shipboard ADCP and TSG survey plus a few drifter deployments. We heavily used the Barents 2.5 operational Norwegian numerical model to guide us, which ended up having remarkably accurate surface temperature and salinity features. We ascertained that there was a region of submesoscale 'soup' between the northbound warm Atlantic water that was primarily on the east side of the ridge, and the Greenland basin water to the west. The soup region appeared to have a rich field of submesoscale eddy stirring, and a wide range of intermediate water

properties between the Atlantic and Greenlandic water masses. Currents in the soup region were modest, and eddying. We decided that this would make an ideal location to center at least the first week of our experiment. We deployed the DBASIS in the middle of this region, hoping that it would not travel far and thus be able to act as an anchor for both acoustic experiments (with its sound source) and an anchoring time series to contextualize shipboard and glider surveys in the vicinity. Conveniently we were able to place it between the acoustic and receiver moorings as well. A few test profiles with the MOD RBR CTD shows lots of structure, including a dramatic sub-surface temperature maximum, whose T-S properties match those of the Atlantic water to the East.

13-14 November: Diamond shipboard profiling survey. To get a feel for the variability of sub-surface structure, we conducted a diamond-shaped shipboard profiling survey roughly centered on the DBASIS. The first three legs were conducted with the CTD, and the last (S-W) leg was conducted with the Epsi-fish microstructure profiler and bow chain. A short test of the V-Wing system was also conducted. The Bergen "Urd" glider was deployed and sent on a wider-scale survey of this region, while the "Electra" glider continues to maintain the line between the source and receiver mooring.

15 November: Acoustics Intensive, Part I. With at least a preliminary understanding of the water mass structure and associated sound speed patterns in the region, we spent the full day setting up an acoustics experiment. The Pecos receiver mooring was placed into continuous record mode for 12 hours. A series of acoustic receiving assets were then deployed in roughly a 12-mile line stretching due West of DBASIS. The same line was then re-occupied with a series of stations in which the ship-board source was lowered and set to transmit. Finally the line was occupied with a CTD profiling transect to map out the T-S-Sound Speed properties. During this time winds were very weak and waves were small.

16 November: Long along-channel line. Up to this point the profiling sections have been a little piece-meal. To complement the diamond shape and get a good look at turbulence in this spicy soup area, we conducted a ~50 mile line roughly along the Jan Mayen channel, starting near the island tip and transiting all the way to the warm Atlantic water at the East end of the channel.

17-19 November: Recoveries. DBASIS was having trouble profiling, seems the upper WW didn't have enough buoyancy, such that it was going slower and slower and starting to stall for hours. So on 17 Nov we recovered it, changed the buoyancy, and re-deployed in the evening. Overnight we did four shipboard CTD/LADCP profiles near the southern mooring array. On the 18th and 19th we recovered all four moorings smoothly, with more CTDs on the evening in between.

19 November: V-wing. To look at small-scale horizontal structures, we conducted a survey along roughly a 12-mile, along-channel line that has the v-wing and bow chain one direction (4 knots) and the the bow chain and epsi profiling back the other direction at 2 knots. The idea is that we could potentially calculate a poor mans chi with the thermistors, and then compare with

the microstructure, and/or see how the phenomenology of detailed horizontal variability at order meters to tens of meters relates to microstructure estimates of chi and epsilon.

20 November: Acoustics Intensive, Part II. Similar to the previous survey, except now the drifting assets with hydrophones have dispersed further. As with the survey on 15 Nov, the ship-board source was lowered at multiple locations, followed by a ctd profiling survey. The evening was spent recovering and to some extent re-deploying drifting assets in advance of the coming storm.

21 November: waiting for the storm. With DBASIS moving towards the warm side of the front, we relocated on the cold side, to microstructure profile as long as we could and be able to compare/contrast the mixed layer deepening in two nearby but quite different stratifications. Swifts were deployed by both DBASIS and the ship-profiling areas. Surprisingly, we were able to keep going for a full 24 hours.

22-23 November, winter cometh. Hiding behind Jan Mayen.

24-25 November, post-storm sampling. We emerged from hiding mid-day on the 25th to resume sampling. After recovering a SWIFT, we conducted a first cross-channel ctd-profiling survey near Jan Mayen. In this region it appeared that storm mixing had eaten up maybe half of the subsurface warm layer (presumably releasing that heat to the atmosphere), but by the time we arrived it was already starting to laterally restratify/slump. We continued sampling all the way south to DBASIS, noting that on the warm side of the front (that DBASiS had migrated to), storm-driven mixed layer deepening seemed to have gone much deeper and was slower to restratify, owing presumably to fewer lateral density gradients on that side.

25 November. Acoustics Intensive part 3. We recovered a bunch of drifting assets in order to redeploy them in an acoustics experiment going due north from DBASIS, across a temperature front. As with the other intensives, this was followed by an occupation with the ship-deployed sound source, then we ended with an epsi-bow chain back northward along the same line and a v-wing + bow chain southward along the line.

26 November. Final surveying associated with the acoustics intensive line was completed by lunch-time, and sweep-up recover of all instruments begins.

27 November. Finished picking up the last drifters early in the am, started transit to Tromsø.

29 November 0830. Arrived at the dock.

Swift Deployments

| SWIFT # | Deploy | 2023 | Time UTC | Latitude | Longitude | Recovery | 2023 | Time UTC | Latitude | Longitude |
|----------|--------|--------|----------|-------------|-------------|----------|--------|----------|-------------|-------------|
| SWIFT 24 | | 13-Nov | 16:38 | 71° 05.263' | -7° 41.727' | | 18-Nov | 17:49 | 70° 35.910' | -8° 46.861' |
| SWIFT 22 | | 13-Nov | 18:40 | 71° 05.404' | -7° 35.705' | | 18-Nov | 19:30 | 70° 30.153' | -7° 14.329' |
| SWIFT 23 | | 13-Nov | 19:50 | 71° 05.316' | -7° 24.835' | | 18-Nov | 18:20 | 70° 33.450' | -8° 50.409' |
| SWIFT 25 | | 13-Nov | 20:55 | 71° 05.225' | -7° 12.421' | | 14-Nov | 17:25 | 70° 56.221' | -7° 17.569' |
| SWIFT 26 | | 14-Nov | 19:35 | 70° 55.474' | -7° 28.324' | | 20-Nov | 18:20 | 70° 57.925' | -8° 01.474' |
| SWIFT 13 | | 15-Nov | 8:04 | 71° 04.003' | -6° 42.570' | | 20-Nov | 22:20 | 70° 38.276' | -8° 56.863' |
| SWIFT 27 | | 15-Nov | 8:07 | 71° 04.003' | -6° 42.570' | | 17-Nov | 12:00 | 71° 03.100' | -7° 05.341' |
| SWIFT 16 | | 15-Nov | 8:38 | 71° 03.996' | -6° 51.671' | | 20-Nov | 23:30 | 70° 44.958' | -7° 13.776' |
| SWIFT 15 | | 15-Nov | 9:01 | 71° 03.977' | -6° 57.882' | | 20-Nov | 20:47 | 70° 48.253' | -7° 20.103' |
| SWIFT 28 | | 15-Nov | 9:40 | 71° 04.025' | -7° 07.665' | | 15-Nov | 18:30 | 71° 04.196' | -8° 51.672' |
| SWIFT 17 | | 15-Nov | 11:42 | 71° 04.022' | -7° 07.670' | | 15-Nov | 19:00 | 71° 03.165' | -8° 54.066' |
| SWIFT 25 | | 15-Nov | 19:15 | 71° 03.400' | -8° 53.723' | | 18-Nov | 17:00 | 70° 39.944' | -8° 55.872' |
| SWIFT 17 | | 17-Nov | 14:20 | 71° 05.745' | -7° 42.426' | | 25-Nov | 17:30 | 70° 21.801' | -7° 50.637' |
| SWIFT 28 | | 17-Nov | 14:22 | 71° 05.607' | -7° 42.423' | | 21-Nov | 13:30 | 71° 14.243' | -8° 49.788' |
| SWIFT 23 | | 19-Nov | 21:00 | 70° 55.503' | -7° 42.056' | | 27-Nov | 7:15 | 70° 52.291' | -5° 45.799' |
| SWIFT 15 | | 21-Nov | 4:30 | 71° 05.409' | -7° 10.655' | | 25-Nov | 16:15 | 70° 10.928' | -7° 42.080' |
| SWIFT 22 | | 21-Nov | 4:34 | 71° 05.360' | -7° 09.631' | | 26-Nov | 13:45 | 70° 12.260' | -7° 26.998' |
| SWIFT 13 | | 21-Nov | 7:30 | 71° 22.012' | -8° 30.496' | | 24-Nov | 11:45 | 70° 57.408' | -8° 34.716' |
| SWIFT 24 | | 21-Nov | 7:35 | 71° 21.780' | -8° 30.253' | | 26-Nov | 19:45 | 70° 30.472' | -8° 48.359' |
| SWIFT 17 | | 25-Nov | 18:45 | 70° 22.626' | -7° 38.632' | | 26-Nov | 14:00 | 70° 14.235' | -7° 34.158' |
| SWIFT 13 | | 25-Nov | 19:30 | 70° 25.541' | -7° 38.328' | | 26-Nov | 16:30 | 70° 19.896' | -7° 28.274' |
| SWIFT 16 | | 25-Nov | 19:50 | 70° 27.594' | -7° 38.621' | | 26-Nov | 17:05 | 70° 20.993' | -7° 28.151' |

CTD/LADCP stations:

| Station # | Longitude (deg min) | Latitude (deg min) | Time (UTC) |
|-----------|---------------------|--------------------|----------------------|
| 311 | 06 26.72 W | 70 50.48 N | Nov 18 2023 01:25:17 |
| 312 | 06 25.62 W | 70 50.82 N | Nov 18 2023 02:22:31 |
| 313 | 06 24.83 W | 70 50.99 N | Nov 18 2023 03:08:10 |
| 314 | 06 24.41 W | 70 51.14 N | Nov 18 2023 04:03:58 |
| 315 | 06 24.10 W | 70 51.33 N | Nov 19 2023 00:14:20 |
| 316 | 06 23.54 W | 70 51.38 N | Nov 19 2023 01:24:35 |
| 317 | 06 22.68 W | 70 51.63 N | Nov 19 2023 02:49:28 |
| 318 | 06 17.70 W | 71 12.80 N | Nov 19 2023 06:39:45 |

Bow Chain Deployments

| | date start | date end | Deployment notes |
|----------------------|-------------------|-----------------|------------------------------------|
| deployment 1 | 11/14/23 08:23 | 11/14/23 15:30 | First deployment, with Epsi |
| deployment 2 | 11/16/23 15:50 | 11/17/23 06:00 | Long Epsi deployment along channel |
| deployment 3a | 11/19/23 17:30 | 11/19/23 23:45 | V-Wing deployment, |
| deployment 3b | 11/19/23 23:50 | 11/20/23 05:10 | Epsi deployment |

V-Wing Deployments

14th November 2023

First test deployment was attempted on 14/11/23, beginning at 17.30Z. Solo Ts and Duets were enabled the day before, and concertos and XR420s were filled with batteries, dessicant and o-rings were checked/greased, bales were attached and wings were attached to the concertos and the two XR420 TCPs (10 instruments). In the hour before the deployment the concertos and XR420s were set to begin recording before being taken out on deck. The ADCP was enabled with the file AD2CP_500kHz_103323_NORSE_1.deploy using a blanking distance of 0.5 m and a cell size of 2 m, and there were no connection issues to the sig500.

We secured the first solo T (serial number 76103) using a single 75lb rated ziptie poked through the spectra, however on recovery this ziptie had sheared off. Subsequent solos and duets were fastened with two zipties, and the final three were also taped directly to the spectra using electrical tape in addition to the two zipties. The planned deployment of solo Ts along the chain was not possible due to the tension within the spectra, so we used only the available loops in the line. The 300 m spectra was paid out until the shackle holding it was in the water, about 30 m back from the end of the ship. Deployment was made at 4 kn and the ship maintained 4kn for 30 minutes. We then made a turn with a turn radius of around 1nm turning 180 degrees to test the turning capabilities of the towed line. The ship then sped up to 6 kn over ground for 20 minutes before recovering the instrument.

| Position along line from V-Wing | Instrument number | Serial Number | Instrument |
|---------------------------------|-------------------|---------------|-------------------|
| 0.0 | | | Sig500 |
| 5.0 | 2 | 200740 | Concerto, WHOI |
| 12.5 | 5 | 66098 | Concerto, WHOI |
| 20.0 | 8 | 60559 | Concerto, Scripps |
| 27.5 | 11 | 60183 | Concerto, Scripps |
| 35.0 | 14 | 60281 | Concerto, Scripps |
| 42.5 | 17 | 60523 | Concerto, Scripps |
| 50.0 | 20 | 60558 | Concerto, Scripps |
| 57.5 | 23 | 65798 | Concerto, Scripps |
| 65.0 | 26 | 17563 | XR420 TC |
| 72.5 | 29 | 15246 | XR420 TC |
| 80.0 | 35 | 15225 | XR420 TC |
| 87.5 | 41 | 17263 | XR420 TCP |
| 95.0 | 47 | 17561 | XR420 TC |
| 102.5 | 53 | 17559 | XR420 TC |
| 110.0 | 59 | 13249 | XR420 TCP |
| 117.5 | 32 | 204313 | Duet, WHOI |
| 125.0 | 38 | 203184 | Duet, Scripps |
| 132.5 | 3 | 76110 | Solo T, WHOI |
| 140.0 | 4 | 76102 | Solo T, WHOI |
| 147.5 | 6 | 76104 | Solo T, WHOI |

19th November 2023

Our second deployment took place on the 19/11/23, around 18.30Z. The concertos and XR420s were enabled during the afternoon in preparation for the deployment, as was the Signature500 ADCP. Due to an inability to communicate with the ADCP, we reconnected the battery to set it sampling in the same mode as in the first deployment, then later took out the SD card to download data.

Solo Ts and Duets were added in large numbers to this deployment, using additional loops that were added to the spectra the day before. Loops were added every 1.5 m, starting at 2 m from the V-Wing, all the way up to 110 m. Measurements were made using a tape measure, starting from the end of the line that attaches to the V-Wing, and we found that by the time we'd reached the marked loops, we were consistently 10cm off (increasing to 20 cm when the spacing between original loops increased from 7.5 m to 15 m). The solo Ts and Duets were attached to the line with two zipties into the added loops. The loops were made using high strength twine tied with a square knot. The solo Ts and Duets were then taped with electrical tape flat onto the line, with the temperature probe pointing towards the V-Wing, which adds an additional distance offset for the placement of the temperature measurements.

Deployment was made at 4 knots, and took around an hour to fully deploy. We were aiming for a depth of 60-80 m, based on the range of the ADCP, and used the previous deployment to guide the amount of line to let out. We ensured that the loop at 215 m was in the water, about 30 m back from the boat. Before deploying the V-Wing, the bow-chain was deployed in order to get simultaneous measurements with both instrument arrays.

The ship track was maintained in a single direction, aiming to cross over the temperature intrusions and reach the warmer water to the east, whilst keeping a heading that the ship could maintain with the bow

chain in the water. After recovering the V-Wing, we then went back along the same line with the epsilonometer profiling at 2 knots to get comparative measurements of turbulence along the same line. The line was not completed, but there is some coincident data. All the instruments were successfully recovered by around 13.00Z on the 20/11/23, giving a tow of around 40 km in around 6 hours.

| Position along line from V-Wing | Instrument Number | Serial Number | Instrument | Position along line from V-Wing | Instrument Number | Serial Number | Instrument |
|---------------------------------|-------------------|---------------|-------------------|---------------------------------|-------------------|---------------|-------------------|
| -0.45 | 0 | 3717216 | SBE37 | 45.5 | 30 | 2070119 | Solo T, Scripps |
| -0.45 | 0.5 | 3707716 | SBE37 | 47 | 31 | 2070611 | Solo T, Scripps |
| 0 | | | Sig500 | 48.5 | 32 | 207032 | Solo T, Scripps |
| 2 | 1 | 761102 | Solo T, WHOI | 50 | 33 | 40558 | Concerto, Scripps |
| 3.5 | 2 | 761104 | Solo T, WHOI | 51.5 | 34 | 100700 | Solo T, Scripps |
| 5 | 3 | 13249 | XR420-TCP | 53 | 35 | 207065 | Solo T, Scripps |
| 6.5 | 4 | 76110 | Solo T, WHOI | 54.5 | 36 | 100694 | Solo T, Scripps |
| 8 | 5 | 101314 | Solo T, WHOI | 56 | 37 | 207063 | Solo T, Scripps |
| 9.5 | 6 | 761111 | Solo T, WHOI | 57.5 | 38 | 204313 | Duet, Scripps |
| 11 | 7 | 101316 | Solo T, WHOI | 59 | 39 | 77582 | Solo T, Scripps |
| 12.5 | 8 | 60098 | Concerto, WHOI | 60.5 | 40 | 207026 | Solo T, Scripps |
| 14 | 9 | 100037 | Solo T, WHOI | 62 | 41 | 207034 | Solo T, Scripps |
| 15.5 | 10 | 100038 | Solo T, WHOI | 63.5 | 42 | 207036 | Solo T, Scripps |
| 17 | 11 | 101317 | Solo T, WHOI | 65 | 43 | 45798 | Concerto, Scripps |
| 18.5 | 12 | 761108 | Solo T, WHOI | 66.5 | 44 | 207057 | Solo T, Scripps |
| 20 | 13 | 60559 | Concerto, Scripps | 68 | 45 | 207015 | Duet, Scripps |
| 21.5 | 14 | 761109 | Solo T, WHOI | 69.5 | 46 | 209753 | Solo T, Harper |
| 23 | 15 | 100035 | Solo T, WHOI | 71 | 47 | 207010 | Duet, Scripps |
| 24.5 | 16 | 101315 | Solo T, WHOI | 72.5 | 48 | 209745 | Solo T, Harper |
| 26 | 17 | 761106 | Solo T, WHOI | 74 | 49 | 207008 | Duet, Scripps |
| 27.5 | 18 | 60183 | Concerto, Scripps | 75.5 | 50 | 209748 | Solo T, Harper |
| 29 | 19 | 207062 | Solo T, Scripps | 77 | 51 | 203188 | Duet, Scripps |
| 30.5 | 20 | 207043 | Solo T, Scripps | 78.5 | 52 | 209746 | Solo T, Harper |
| 32 | 21 | 207038 | Solo T, Scripps | 80 | 53 | 17582 | XR420 TC |
| 33.5 | 22 | 207051 | Solo T, Scripps | 95 | 54 | 15246 | XR420 TC |
| 35 | 23 | 60281 | Concerto, Scripps | 110 | 55 | 15225 | XR420 TC |
| 36.5 | 24 | 207029 | Solo T, Scripps | 125 | 56 | 203184 | Duet, Scripps |
| 38 | 25 | 207049 | Solo T, Scripps | 140 | 57 | 17263 | XR420 TCP |
| 39.5 | 26 | 207044 | Solo T, Scripps | 155 | 58 | 207012 | Duet, Scripps |
| 41 | 27 | 207039 | Solo T, Scripps | 170 | 59 | 17581 | XR420 TC |
| 42.5 | 28 | 60523 | Concerto, Scripps | 185 | 60 | 82491 | Duet, Scripps |
| 44 | 29 | 207037 | Solo T, Scripps | 200 | 61 | 17559 | XR420 TC |
| | | | | 215 | empty | empty | empty |

26th November 2023

Our third deployment took place on the 26/11/23, starting around 0800Z. The concertos and XR420s were enabled on the afternoon of the 25th in preparation for the deployment. The Signature 500 ADCP owned by the UOP group was no longer switching to redeploy mode after plugging in the battery, so could not be deployed. Instead, we borrowed the Signature 500 ADCP from Jim Thompson's group that had recently come off the mooring. It was enabled using the same settings as were chosen for the previous deployments. However, although it was pinging, it was set to 'online' mode so was not recording and we did not manage to collect any ADCP data for this deployment.

Deployment was made at 4 knots and took around an hour to deploy. We were aiming for the same depth as in deployment 2, using the same instrument arrangement (but this time including instrument

55 which was previously missing, and switching out Instrument 53). The line was let out until the final instrument at 215 m from the V-Wing was in the water (about 30 m back from the boat).

| Position along line from V-Wing | Instrument Number | Serial Number | Instrument | Position along line from V-Wing | Instrument Number | Serial Number | Instrument |
|---------------------------------|-------------------|---------------|-------------------|---------------------------------|-------------------|---------------|-------------------|
| -0.45 | 0 | 3717216 | SBE37 | 45.5 | 30 | 207019 | Solo T, Scripps |
| -0.45 | 0.5 | 3707716 | SBE37 | 47 | 31 | 207061 | Solo T, Scripps |
| 0 | No data | No data | No data | 48.5 | 32 | 207022 | Solo T, Scripps |
| 2 | 1 | 76102 | Solo T, WHOI | 50 | 33 | 60558 | Concerto, Scripps |
| 3.5 | 2 | 76104 | Solo T, WHOI | 51.5 | 34 | 100700 | Solo T, Scripps |
| 5 | 3 | 13249 | XR420 TCP | 53 | 35 | 207065 | Solo T, Scripps |
| 6.5 | 4 | 76110 | Solo T, WHOI | 54.5 | 36 | 100694 | Solo T, Scripps |
| 8 | 5 | 101314 | Solo T, WHOI | 56 | 37 | 207043 | Solo T, Scripps |
| 9.5 | 6 | 76111 | Solo T, WHOI | 57.5 | 38 | 204313 | Duet, Scripps |
| 11 | 7 | 101315 | Solo T, WHOI | 59 | 39 | 77562 | Solo T, Scripps |
| 12.5 | 8 | 66998 | Concerto, WHOI | 60.5 | 40 | 207026 | Solo T, Scripps |
| 14 | 9 | 100037 | Solo T, WHOI | 62 | 41 | 207034 | Solo T, Scripps |
| 15.5 | 10 | 100038 | Solo T, WHOI | 63.5 | 42 | 207036 | Solo T, Scripps |
| 17 | 11 | 101317 | Solo T, WHOI | 65 | 43 | 65798 | Concerto, Scripps |
| 18.5 | 12 | 76108 | Solo T, WHOI | 66.5 | 44 | 207057 | Solo T, Scripps |
| 20 | 13 | 60359 | Concerto, Scripps | 68 | 45 | 207015 | Duet, Scripps |
| 21.5 | 14 | 76109 | Solo T, WHOI | 69.5 | 46 | 209753 | Solo T, Harper |
| 23 | 15 | 100035 | Solo T, WHOI | 71 | 47 | 207010 | Duet, Scripps |
| 24.5 | 16 | 101315 | Solo T, WHOI | 72.5 | 48 | 209745 | Solo T, Harper |
| 26 | 17 | 76106 | Solo T, WHOI | 74 | 49 | 207008 | Duet, Scripps |
| 27.5 | 18 | 60183 | Concerto, Scripps | 75.5 | 50 | 209748 | Solo T, Harper |
| 29 | 19 | 207062 | Solo T, Scripps | 77 | 51 | 203188 | Duet, Scripps |
| 30.5 | 20 | 207043 | Solo T, Scripps | 78.5 | 52 | 209746 | Solo T, Harper |
| 32 | 21 | 207038 | Solo T, Scripps | 80 | 53 | 15247 | XR420 TC |
| 33.5 | 22 | 207051 | Solo T, Scripps | 95 | 54 | 15246 | XR420 TC |
| 35 | 23 | 60281 | Concerto, Scripps | 110 | 55 | 15223 | XR420 TC |
| 36.5 | 24 | 207029 | Solo T, Scripps | 125 | 56 | 15225 | XR420 TC |
| 38 | 25 | 207049 | Solo T, Scripps | 140 | 57 | 203184 | Duet, Scripps |
| 39.5 | 26 | 207044 | Solo T, Scripps | 155 | 58 | 17263 | XR420 TCP |
| 41 | 27 | 207039 | Solo T, Scripps | 170 | 59 | 207012 | Duet, Scripps |
| 42.5 | 28 | 60523 | Concerto, Scripps | 185 | 60, no data | 17561 | XR420 TC |
| 44 | 29 | 207037 | Solo T, Scripps | 200 | 61 | 82491 | Duet, Scripps |
| | | | | 215 | 62 | 17559 | XR420 TC |